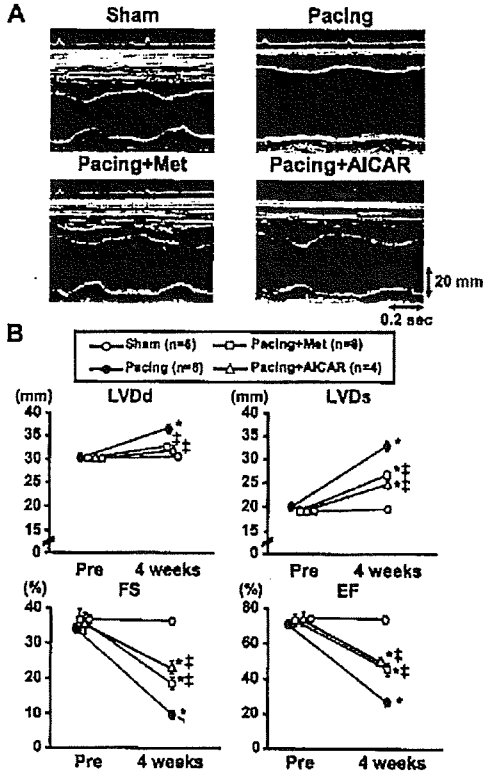

Figure 3. Effect of metformin on echocardiographic parameters. A, Representative M-mode echocardiograms obtained 4 weeks after sham surgery or after RV pacing. B, Echocardiographic parameters before and after sham surgery or after RV pacing in the sham group (n=6), pacing group (n=8), pacing plus metformin group (n=8), and pacing plus AICAR group (n=4). Values are mean±SEM. LVDd indicates LV end-diastolic dimension; LVDs, LV end-systolic dimension; LVFS, LV fractional shortening; and LVEF, LV ejection fraction. *$P<0.01$ vs sham group; ‡$P<0.01$ vs pacing group.

Importantly, the percentage of TUNEL-positive cells to total cells in LV myocardium in the pacing group increased compared with that in the sham group, which was blunted by treatment with either metformin or AICAR (Figure 5A through 5E).

Consistent with previous data,[17] no significant differences were found in body weight, the ratio of LV plus septal weight to body weight, and the ratio of RV weight to body weight among all groups (the Table).

To explore established markers of cardiac failure, we analyzed LV myocardial expression of the atrial natriuretic peptide and brain natriuretic peptide genes, which showed an increase in the pacing group, whereas metformin significantly suppressed this increase (Figure 6A and 6B). Metformin also significantly reduced the levels of angiotensin II and norepinephrine compared with the pacing group (the Table).

Pedometer counts were significantly reduced in the pacing group compared with the sham group, suggesting that heart failure led to reduced physical activities (the Table). Metformin increased the pedometer count compared with that in the pacing group. No differences in body fat were found among all groups (the Table).

Cardiac Molecular Parameters

To assess the molecular basis of the improvement in cardiac performance achieved by metformin administration for 4 weeks, we examined the collagen volume fraction in LV myocardium after staining with Masson's trichrome stain. Metformin reduced the collagen volume fraction compared with the pacing group (Figure 6C and 6D). To further investigate the mechanism of this antifibrotic effect of metformin, we examined the level of transforming growth factor-β1 (TGF-β1) mRNA associated with fibrosis in canine LV myocardium 4 weeks after pacing. Metformin suppressed the increase in TGF-β1 mRNA expression (Figure 6E).

AMPK was phosphorylated in the pacing group, and its phosphorylation was significantly enhanced by administration of metformin (Figure 7A and 7B). Phosphorylation was used as an index of enzymatic activity because AMPK is activated by phosphorylation.[18] This increase in AMPK phosphorylation was accompanied by augmented phosphorylation of acetyl-CoA carboxylase (ACC; a downstream target of AMPK) at Ser-79 (Figure 7A and 7C). Endothelial NO synthase (eNOS) also showed an increase in phosphorylation at Ser-1177 with metformin treatment (Figure 7A and 7D). Furthermore, metformin significantly upregulated eNOS mRNA expression and increased ΔNO (the difference between the plasma NO level before and after 4 weeks of RV pacing) compared with the pacing group (Figure 8A and 8B).

To investigate the level of insulin signaling in the heart, we examined the phosphorylation of Akt in the left ventricles in all groups. Significant increases were found in phosphorylation of Akt at Ser-473 in the pacing group compared with the sham group, and such increases were blunted by either metformin or AICAR treatment (Figure 8C and 8D).

Plasma and Cardiac Metabolic Parameters

To investigate whether activation of AMPK by metformin influenced metabolic parameters in the periphery or the heart, we assessed glucose and lipid metabolism after 4 weeks of pacing. Plasma free fatty acids tended to increase in the pacing group compared with the sham group, although no statistically significant difference was found. Fasting plasma levels of both glucose and lactate were similar among all groups (the Table). Both the fasting plasma insulin level and the homeostasis model assessment–insulin resistance value were significantly increased in the pacing group, whereas metformin reduced both parameters until they were similar to those of the sham group (the Table).

In the heart, both glucose extraction and the arterial–coronary sinus difference were increased in the pacing group compared with the sham group (the Table). In the pacing group, the free fatty acids extraction was not increased, but the arterial–coronary sinus difference tended to increase compared with the sham group (the Table). Lactate extraction and the arterial–coronary sinus difference were similar among all groups (the Table).

AICAR Mimics the Effect of Metformin in This Canine Pacing Model

To further confirm that activation of AMPK contributed to inhibition of the progression of heart failure, we administered

Table. Characteristics of the Dogs at 4 Weeks

	Sham Group (n=6)	Pacing Group (n=8)	Pacing+Metformin Group (n=8)	Pacing+AICAR Group (n=4)
Organ weight				
Body weight, kg	9.5±0.2	9.4±0.2	9.7±0.1	9.6±0.3
LV+septal weight, g	42±0.6	47.3±1.2	43.6±0.9	44.8±1.3
LV+septal weight/body weight ratio, g/kg	4.4±0.1	5.0±0.1	4.5±0.1	4.7±0.2
RV weight, g	14.7±0.5	15.6±0.6	15.0±1.2	14.7±1.0
RV weight/body weight ratio, g/kg	1.5±0.1	1.7±0.1	1.5±0.1	1.5±0.1
Hemodynamic parameters				
Mean aortic pressure, mm Hg	105±5	109±2	100±2	97±3.3
Heart rate, bpm	118±5	136±4	128±5	126±3.6
Cardiac output, L/min	2.6±0.1	1.6±0.1*	2.2±0.3†	2.2±0.3†
Systemic vascular resistance, dynes · s · cm^{-5}	3317±189	4769±235*	3775±334†	3763±237†
Plasma metabolic parameters				
Fasting glucose, mmol/L	5.3±0.3	5.3±0.1	5.3±0.1	5.3±0.2
Fasting insulin, μU/mL	14.2±3.3	67.6±13.7*	18.9±7.3†	24.4±10.5†
HOMA-IR	3.4±0.1	15.8±0.1*	4.4±0.1†	5.8±0.1†
Free fatty acids, μmol/L	305±67	716±68	554±101	595±69
Lactate, mmol/L	1.4±0.2	1.5±0.2	1.5±0.1	1.4±0.1
Cardiac metabolic substrates				
Glucose				
Arterial, mmol/L	5.8±0.1	6.4±0.2	6.6±0.1	6.6±0.4
Arterial–coronary sinus difference, mmol/L	0.6±0.1	1.6±0.3*	0.9±0.1	1.1±0.3
Extraction rate, %	10.5±1.2	28.6±4.7*	13.3±1.8	17.7±4.7
Free fatty acids				
Arterial, mmol/L	213.5±44.9	532.3±98.5*	312.8±56.6	294.5±22.8
Arterial–coronary sinus difference, mmol/L	90.4±13.2	153.7±20.6	99.0±9.1	103.2±20.6
Extraction rate, %	47.5±9.2	29.9±2.8	33.9±5.1	36.9±8.6
Lactate				
Arterial, mmol/L	1.8±0.1	1.9±0.3	2.3±0.7	1.8±0.8
Arterial–coronary sinus difference, mmol/L	1.2±0.3	1.0±0.2	1.3±0.5	1.1±0.4
Extraction rate, %	62.6±16.0	48.2±3.8	55.0±12.2	61.8±6.9
Plasma neurohormone levels				
Norepinephrine, pg/mL	34.9±13.0	195.9±21.3*	59.2±11.2†	79.3±8.9†
Angiotensin II, pg/mL	34.7±15.0	153.6±24.3*	78.1±14.8†	73.4±11.8†
Body fat and activity				
Body fat, %	13.7±1.2	18.7±2.9	16±1.2	14.3±0.8
Pedometer count	88 783±2899	64 541±2530*	78 423±3292†	77 716±1472†

HOMA-IR indicates homeostasis model assessment–insulin resistance. Values are mean±SEM.
*$P<0.05$ vs the sham group; †$P<0.05$ vs the pacing group.

another AMPK activator (AICAR at a dose of 5 mg/kg SC every other day) to dogs. As expected, AICAR reproduced the effects of metformin in this canine pacing model (Figures 3 through 8).

Discussion

To the best of our knowledge, this is the first study to demonstrate clearly that long-term (not short-term) oral administration of metformin, which is used as an antidiabetic agent worldwide, inhibits cardiac remodeling and prevents the progression of heart failure in dogs, along with increases in AMPK activation and NO production. Of course, we and others have previously shown that in rodent either AMPK activation or NO production attenuates myocardial ischemia/reperfusion injury in the ischemic model[7–9] and prevents cardiac remodeling in the pressure overload model.[11,12,19,20] However, it has been unclear whether AMPK or NO can modulate cardiac remodeling and inhibit the progression of heart failure in a canine model with another pathogenic mechanism that is not an ischemic or a pressure overload heart failure model. Therefore, we used a rapid pacing-induced heart failure dog model, which is considered to be similar to human dilated cardiomyopathy[21,22] and can be superimposed on translational study for human heart failure.

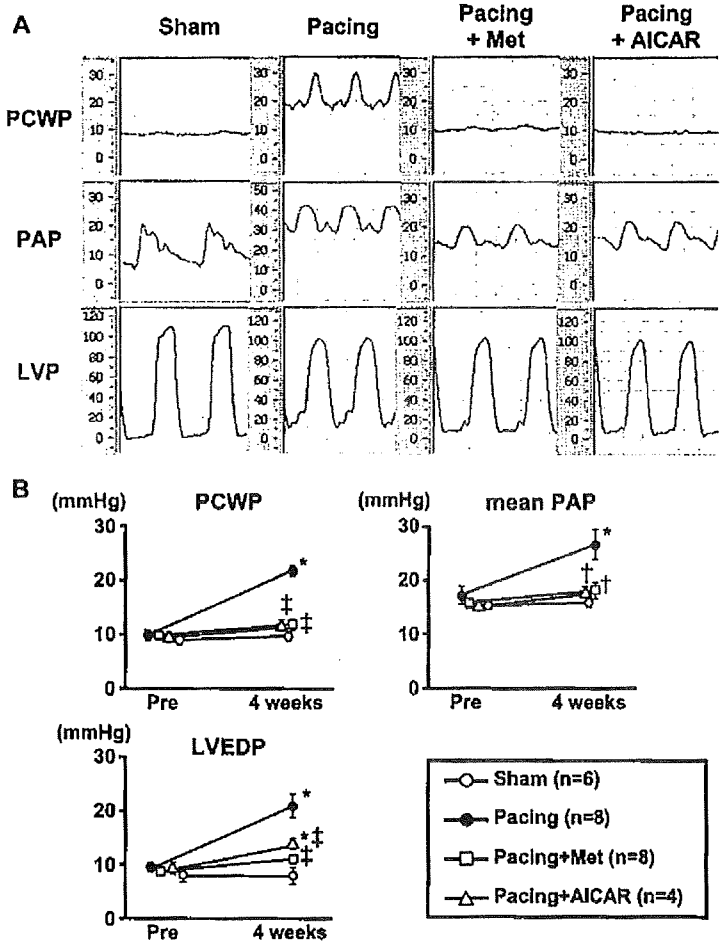

Figure 4. Effect of metformin on hemodynamic parameters. A, Representative graphs of hemodynamic parameters obtained at 4 weeks. B, Hemodynamic parameters before and after the 4-week study period in the sham (n=6), pacing (n=8), pacing plus metformin (n=8), and pacing plus AICAR (n=4) groups. Values are mean±SEM. PAP indicates pulmonary artery pressure; PCWP, pulmonary capillary wedge pressure; and LVEDP, LV end-diastolic pressure. *$P<0.05$ vs sham group; †$P<0.05$ vs pacing group; ‡$P<0.01$ vs pacing group.

Furthermore, we provide sufficient insight because dogs can be monitored more precisely for hemodynamic data than rodents.

Possible Cardioprotective Mechanism of Metformin Mediated via AMPK

Metformin has previously been shown to reduce high fat–induced apoptosis,[23] and AMPK has been reported to protect against hypoxic apoptosis in cardiomyocytes through attenuation of endoplasmic reticulum stress.[24] Consistent with these previous reports, we confirmed that metformin could ameliorate oxidative stress–induced apoptosis in cardiomyocytes. This effect was blunted by compound C, an AMPK inhibitor, suggesting that activation of AMPK was responsible for the inhibition of cardiomyocyte apoptosis. Furthermore, using a dog model, we demonstrated that metformin ameliorated the progression of heart failure induced by rapid RV pacing and decreased apoptosis in the LV myocardium, as indicated by TUNEL staining. Interestingly, AICAR, another AMPK activator, had effects almost identical to those of metformin, supporting that the activation of AMPK contributed to the observed cardioprotective effect. Indeed, AICAR also has been reported to reduce myocardial ischemia/reperfusion injury in humans and animals.[25,26] What processes following AMPK activation are involved in cardioprotection?

The first possibility is enhancement of NO production. Recchia et al[27] reported that basal cardiac NO release is decreased in dogs with heart failure induced by rapid pacing. We found that the difference in plasma NO levels between baseline and 4 weeks of RV pacing was significantly increased by metformin treatment compared with the pacing group. Metformin has been shown to phosphorylate AMPK at Thr-172 in cardiomyocytes and murine hearts,[4,5] whereas AMPK is known to phosphorylate eNOS at Ser-1177 in rat hearts,[28] resulting in an increase in NO production. Indeed, a recent report has indicated that short-term metformin treatment protects against myocardial infarction via AMPK-eNOS–mediated signaling in mice.[7] Other studies have suggested involvement of the AMPK-eNOS pathway in the response of endothelial cells to shear stress,[29] metformin,[30] and statins.[31] Consistent with these reports, we found that either metformin or AICAR promoted the phosphorylation of eNOS at Ser-1177 and increased both mRNA and protein levels of eNOS, possibly leading to increased plasma NO levels and reduced systemic vascular resistance. Although the precise mechanism of the effects of phosphorylation of AMPK by either metformin or AICAR on eNOS protein expression is not clear, these findings suggest that metformin or AICAR increased NO production, which improves endothelial

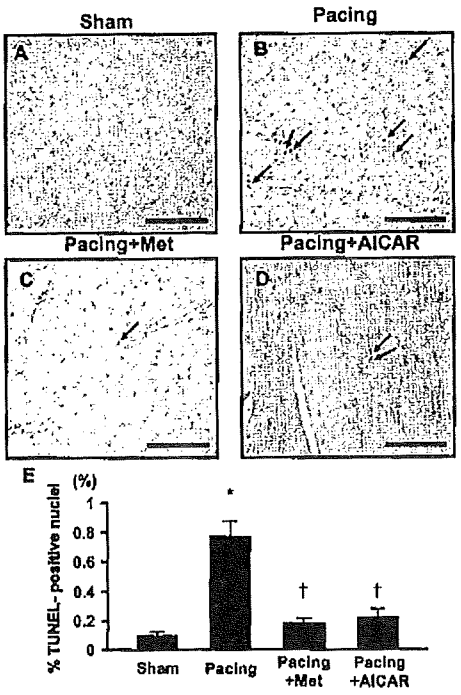

Figure 5. TUNEL staining of canine hearts at 4 weeks. Representative examples of TUNEL-stained hearts from sham (A), pacing (B), pacing plus metformin (C), and pacing plus AICAR (D) groups. Arrows indicate TUNEL-positive nuclei (brown). Scale bar=100 μm. E, Quantitative data on the percentage of TUNEL-positive nuclei to total cell nuclei. *P<0.05 vs sham group; †P<0.05 vs pacing group.

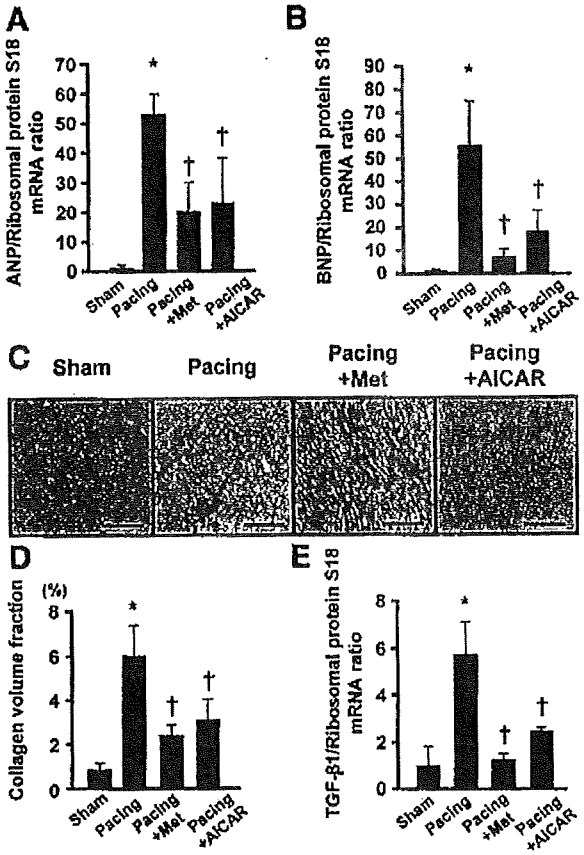

Figure 6. Natriuretic peptide expression, cardiac collagen volume fraction, and TGF-β1 expression. A, B, and E, Quantitative real-time reverse-transcriptase polymerase chain reaction analysis of myocardial atrial natriuretic peptide (ANP), brain natriuretic peptide (BNP), and TGF-β1 expression, respectively. The mRNA values were corrected for the ribosomal protein S18 mRNA level. The sham group was arbitrarily assigned a value of 1.0. Results are mean±SEM. Representative results from 3 independent experiments are shown. *P<0.05 vs sham group; #P<0.05 vs pacing group. C, Representative histological appearance of LV myocardium stained with Masson's trichrome stain (light blue). Scale bar=100 μm. D, Collagen volume fraction in the LV myocardium. Values are mean±SEM. *P<0.05 vs sham group; †P<0.05 vs pacing group.

function. NO is believed to have various cardioprotective effects.[16] Therefore, enhancement of NO production by metformin via activation of AMPK may have contributed to alleviating the progression of heart failure induced by rapid RV pacing.

The second possibility is related to the improvement in insulin resistance. It is known that insulin resistance is associated with the progression of chronic heart failure, whereas chronic heart failure may provoke insulin resistance by increasing sympathetic activity, activating the renin-angiotensin system, or both.[32,33] We found that rapid RV pacing for 4 weeks induced heart failure and that metformin treatment improved insulin resistance (estimated by homeostasis model assessment–insulin resistance) compared with the pacing group, suggesting that the beneficial effect of metformin on heart failure mediated via AMPK may have been due in part to an improvement in insulin resistance.

The third possibility is the metabolic effects of AMPK activation. Both metformin and AICAR are reported to increase glucose extraction in heart,[34,35] which may decrease the severity of the failing hearts. However, we found a 2- to 3-fold increase in myocardial glucose extraction of pacing dogs, and metformin returned glucose extraction to the value of the sham group. Numerous studies have shown a switch from free fatty acids to glucose as the primary energy substrate in humans and animals with advanced heart failure,[27,36–38] suggesting that the reduction in glucose extraction by the improvement in heart failure by AMPK activation is likely to be greater than the induction of glucose extraction by direct activation of AMPK. The possibility exists that AMPK-induced glucose extraction triggers the improvement in heart failure, followed by the restoration of metabolic switch. On the other hand, we found that the net free fatty acids extraction of the pacing group tended to increase despite no statistical significance, which is consistent with the report by Paolisso et al[39] that myocardial free fatty acids extraction increased in patients with congestive heart failure[39] but is contrary to the reports of the metabolic switch.[27,36–38] The metabolic switch may differ in relatively acute or chronic heart failure and by the severity of heart failure.

The increased phosphorylation of Akt in the pacing group was attenuated in either the pacing plus metformin or the pacing plus AICAR group, suggesting that the levels of activation of insulin signaling decreased in either the

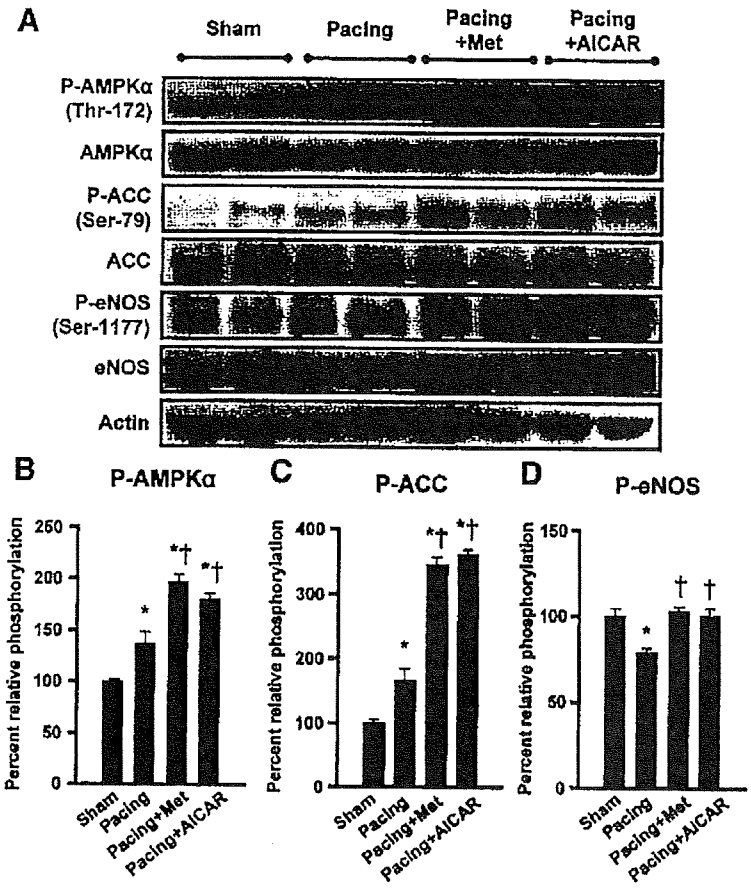

Figure 7. Phosphorylation of AMPKα, ACC, and eNOS in canine hearts after 4 weeks of treatment with or without metformin and AICAR. A, Representative immunoblots of phospho-AMPKα, ACC, and eNOS. B through D, Percentage relative phosphorylation of AMPKα, ACC, and eNOS, respectively. Values are mean±SEM. Representative results from 3 independent experiments are shown. *$P<0.05$ vs sham group; †$P<0.05$ vs pacing group.

metformin- or AICAR-treated group. Considering that glucose extraction was decreased in the pacing plus metformin and pacing plus AICAR groups and that AMPK was phosphorylated by either metformin or AICAR, which may increase in glucose extraction in the heart, the present data may be contradictory, but they are not contradictory when we consider the changes in phosphorylated Akt. The reason is that in this pacing-induced canine heart failure model, glucose extraction in the heart was influenced predominantly by insulin resistance, accompanied by the severity of heart failure, rather than AMPK phosphorylation, although further investigation on this issue is needed.

The fourth possibility is the antifibrotic effect of metformin. Several studies have indicated that AMPK activation inhibits protein synthesis through effects on both the eEF-2 and mTOR pathways.[40,41] We demonstrated that no significant difference in ventricular mass existed at autopsy among the groups. This dog pacing model has been reported to preserve wall thickness without hypertrophy or a consistent increase in heart weight, unlike the pressure overload model.[42] We found that metformin attenuated fibrosis and reduced the TGF-β1 mRNA level after 4 weeks of RV pacing compared with the pacing group. Metformin also improved representative markers of heart failure, including LV end-diastolic pressure, brain natriuretic peptide, angiotensin II, and norepinephrine. Although a number of factors may have contributed to the antifibrotic effect of metformin, our data suggest that inhibition of TGF-β1 by metformin has at least some role, resulting in the prevention of heart failure.

Taken together, these data suggest that metformin has a direct cardioprotective effect, has effects on the improvements of peripheral vascular system and insulin resistance, and inhibits fibrosis. All these actions might contribute to the improvement in the pathophysiology of heart failure, although we could not identify the exact role of each factor. It remains to be determined whether these results were a cause or consequence of improved cardiac function, especially in systemic effects of both insulin resistance and systemic vascular resistance.

Study Limitations

We found that the extent of phosphorylation of eNOS decreased despite the increase in the phosphorylated Akt in the pacing-induced failing canine hearts, which may be contradictory to previous reports that the phosphorylation of Akt leads to eNOS phosphorylation.[43,44] Because the signal transduction to modulate eNOS is unclear in the failing myocardium and the pathophysiological role and importance of Akt also are unclear, this discrepancy should be clarified in future studies.[45]

We need to consider the dose of metformin used in the present study, which was at least 3-fold higher than that used clinically. Nevertheless, adverse effects such as hypoglycemia and lactic acidosis were not detected during the experiment.

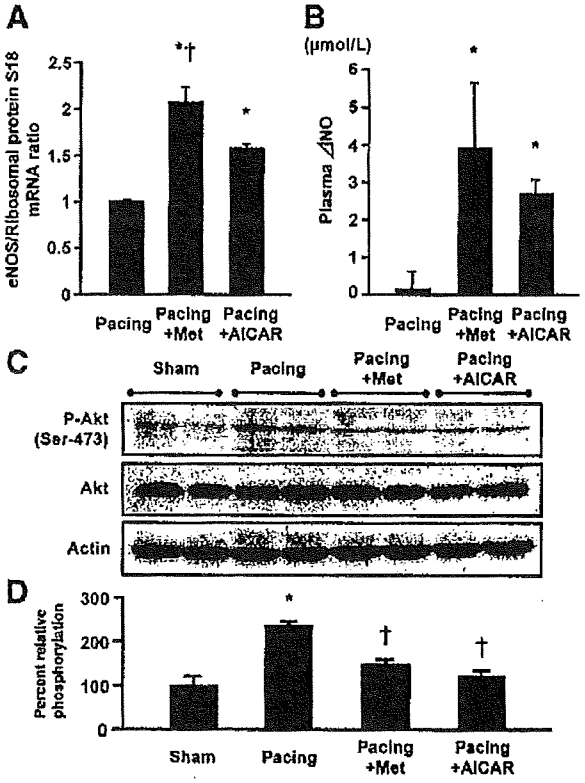

Figure 8. Effect of metformin on eNOS mRNA expression and plasma ΔNO levels, and phosphorylation of Akt in canine hearts. A, Quantitative real-time reverse-transcriptase polymerase chain reaction for eNOS mRNA. The mRNA levels were normalized to ribosomal protein S18 mRNA, and the pacing group was arbitrarily assigned a value of 1.0. B, Plasma ΔNO level after 4 weeks of RV pacing with or without metformin and AICAR administration. Values are mean±SEM. Representative results from 3 independent experiments are shown. *$P<0.05$ vs pacing group; †$P<0.05$ vs pacing plus AICAR group. C, Representative immunoblots of phospho-Akt. D, Percent relative phosphorylation of Akt. Values are mean±SEM. Representative results from 3 independent experiments are shown. *$P<0.05$ vs sham group; †$P<0.05$ vs pacing group.

Conclusions

We demonstrated that metformin prevents the progression of pacing-induced heart failure in dogs, along with the activation of AMPK. Metformin may offer a novel treatment strategy for heart failure.

Acknowledgments

We thank Yoko Horiguchi for her technical assistance; Dr Masafumi Myoishi for his assistance with TUNEL staining; Dr Hai Ying Fu for her assistance with flow cytometry; Dr Hatsue-Ishibashi-Ueda for her assistance with fluorescence microscopy; Dr Kyoko Shioya for her assistance with animal care; Tsunehisa Nakao (Nippon Shinyaku Co Ltd) for providing information about metformin; and the Evidence Finders' Club for their encouragement of this study.

Sources of Funding

This work was supported by grants in aid from the Ministry of Health, Labor, and Welfare–Japan and the Ministry of Education, Culture, Sports, Science and Technology–Japan and grants from the Japan Heart Foundation and the Japan Cardiovascular Research Foundation.

Disclosures

None.

References

1. Effect of intensive blood-glucose control with metformin on complications in overweight patients with type 2 diabetes (UKPDS 34): UK Prospective Diabetes Study (UKPDS) Group. *Lancet.* 1998;352:854–865.
2. Eurich DT, McAlister FA, Blackburn DF, Majumdar SR, Tsuyuki RT, Varney J, Johnson JA. Benefits and harms of antidiabetic agents in patients with diabetes and heart failure: systematic review. *BMJ.* 2007;335:497.
3. Zhou G, Myers R, Li Y, Chen Y, Shen X, Fenyk-Melody J, Wu M, Ventre J, Doebber T, Fujii N, Musi N, Hirshman MF, Goodyear LJ, Moller DE. Role of AMP-activated protein kinase in mechanism of metformin action. *J Clin Invest.* 2001;108:1167–1174.
4. Chan AY, Soltys CL, Young ME, Proud CG, Dyck JR. Activation of AMP-activated protein kinase inhibits protein synthesis associated with hypertrophy in the cardiac myocyte. *J Biol Chem.* 2004;279:32771–32779.
5. Zou MH, Kirkpatrick SS, Davis BJ, Nelson JS, Wiles WG 4th, Schlattner U, Neumann D, Brownlee M, Freeman MB, Goldman MH. Activation of the AMP-activated protein kinase by the anti-diabetic drug metformin in vivo: role of mitochondrial reactive nitrogen species. *J Biol Chem.* 2004;279:43940–43951.
6. Hardie DG. AMP-activated protein kinase: the guardian of cardiac energy status. *J Clin Invest.* 2004;114:465–468.
7. Calvert JW, Gundewar S, Jha S, Greer JJ, Bestermann WH, Tian R, Lefer DJ. Acute metformin therapy confers cardioprotection against myocardial infarction via AMPK-eNOS-mediated signaling. *Diabetes.* 2008;57:696–705.
8. Shibata R, Sato K, Pimentel DR, Takemura Y, Kihara S, Ohashi K, Funahashi T, Ouchi N, Walsh K. Adiponectin protects against myocardial ischemia-reperfusion injury through AMPK- and COX-2-dependent mechanisms. *Nat Med.* 2005;11:1096–1103.
9. Russell RR 3rd, Li J, Coven DL, Pypaert M, Zechner C, Palmeri M, Giordano FJ, Mu J, Birnbaum MJ, Young LH. AMP-activated protein kinase mediates ischemic glucose uptake and prevents postischemic cardiac dysfunction, apoptosis, and injury. *J Clin Invest.* 2004;114:495–503.
10. Tian R, Musi N, D'Agostino J, Hirshman MF, Goodyear LJ. Increased adenosine monophosphate-activated protein kinase activity in rat hearts with pressure-overload hypertrophy. *Circulation.* 2001;104:1664–1669.
11. Shibata R, Ouchi N, Ito M, Kihara S, Shiojima I, Pimentel DR, Kumada M, Sato K, Schiekofer S, Ohashi K, Funahashi T, Colucci WS, Walsh K. Adiponectin-mediated modulation of hypertrophic signals in the heart. *Nat Med.* 2004;10:1384–1389.
12. Liao Y, Takashima S, Maeda N, Ouchi N, Komamura K, Shimomura I, Hori M, Matsuzawa Y, Funahashi T, Kitakaze M. Exacerbation of heart failure in adiponectin-deficient mice due to impaired regulation of AMPK and glucose metabolism. *Cardiovasc Res.* 2005;67:705–713.
13. Bhalla RC, Toth KF, Tan E, Bhatty RA, Mathias E, Sharma RV. Vascular effects of metformin: possible mechanisms for its antihypertensive action in the spontaneously hypertensive rat. *Am J Hypertens.* 1996;9:570–576.
14. Marfella R, Acampora R, Verrazzo G, Ziccardi P, De Rosa N, Giunta R, Giugliano D. Metformin improves hemodynamic and rheological responses to L-arginine in NIDDM patients. *Diabetes Care.* 1996;19:934–939.
15. Katakam PV, Ujhelyi MR, Hoenig M, Miller AW. Metformin improves vascular function in insulin-resistant rats. *Hypertension.* 2000;35:108–112.
16. Rakhit RD, Marber MS. Nitric oxide: an emerging role in cardioprotection? *Heart.* 2001;86:368–372.
17. Komamura K, Shannon RP, Pasipoularides A, Ihara T, Lader AS, Patrick TA, Bishop SP, Vatner SF. Alterations in left ventricular diastolic function in conscious dogs with pacing-induced heart failure. *J Clin Invest.* 1992;89:1825–1838.
18. Lei B, Matsuo K, Labinskyy V, Shanna N, Chandler MP, Ahn A, Hintze TH, Stanley WC, Recchia FA. Exogenous nitric oxide reduces glucose transporters translocation and lactate production in ischemic myocardium in vivo. *Proc Natl Acad Sci U S A.* 2005;102:6966–6971.
19. Li HL, Yin R, Chen D, Liu D, Wang D, Yang Q, Dong YG. Long-term activation of adenosine monophosphate-activated protein kinase

attenuates pressure-overload-induced cardiac hypertrophy. *J Cell Biochem.* 2007;100:1086–1099.
20. Liao Y, Asakura M, Takashima S, Ogai A, Asano Y, Shintani Y, Minamino T, Asanuma H, Sanada S, Kim J, Kitamura S, Tomoike H, Hori M, Kitakaze M. Celiprolol, a vasodilatory beta-blocker, inhibits pressure overload-induced cardiac hypertrophy and prevents the transition to heart failure via nitric oxide-dependent mechanisms in mice. *Circulation.* 2004;110:692–699.
21. Elsner D, Riegger GA. Characteristics and clinical relevance of animal models of heart failure. *Curr Opin Cardiol.* 1995;10:253–259.
22. Lee WL, Chen JW, Ting CT, Ishiwata T, Lin SJ, Kore M, Wang PH. Insulin-like growth factor I improves cardiovascular function and suppresses apoptosis of cardiomyocytes in dilated cardiomyopathy. *Endocrinology.* 1999;140:4831–4840.
23. An D, Kewalramani G, Chan JK, Qi D, Ghosh S, Pulinilkunnil T, Abrahani A, Innis SM, Rodrigues B. Metformin influences cardiomyocyte cell death by pathways that are dependent and independent of caspase-3. *Diabetologia.* 2006;49:2174–2184.
24. Terai K, Hiramoto Y, Masaki M, Sugiyama S, Kuroda T, Hori M, Kawase I, Hirota H. AMP-activated protein kinase protects cardiomyocytes against hypoxic injury through attenuation of endoplasmic reticulum stress. *Mol Cell Biol.* 2005;25:9554–9575.
25. Mangano DT. Effects of acadesine on myocardial infarction, stroke, and death following surgery: a meta-analysis of the 5 international randomized trials: the Multicenter Study of Perioperative Ischemia (McSPI) Research Group. *JAMA.* 1997;277:325–332.
26. Kitakaze M, Takashima S, Minamino T, Node K, Shinozaki Y, Mori H, Kuzuya T, Hori M. Improvement by 5-amino-4-imidazole carboxamide riboside of the contractile dysfunction that follows brief periods of ischemia through increases in ecto-5-nucleotidase activity and adenosine release in canine hearts. *Jpn Circ J.* 1999;63:542–553.
27. Recchia FA, McConnell PI, Bernstein RD, Vogel TR, Xu X, Hintze TH. Reduced nitric oxide production and altered myocardial metabolism during the decompensation of pacing-induced heart failure in the conscious dog. *Circ Res.* 1998;83:969–979.
28. Chen ZP, Mitchelhill KI, Michell BJ, Stapleton D, Rodriguez-Crespo I, Witters LA, Power DA, Ortiz de Montellano PR, Kemp BE. AMP-activated protein kinase phosphorylation of endothelial NO synthase. *FEBS Lett.* 1999;443:285–289.
29. Zhang Y, Lee TS, Kolb EM, Sun K, Lu X, Sladek FM, Kassab GS, Garland T Jr, Shyy JY. AMP-activated protein kinase is involved in endothelial NO synthase activation in response to shear stress. *Arterioscler Thromb Vasc Biol.* 2006;26:1281–1287.
30. Davis BJ, Xie Z, Viollet B, Zou MH. Activation of the AMP-activated kinase by antidiabetes drug metformin stimulates nitric oxide synthesis in vivo by promoting the association of heat shock protein 90 and endothelial nitric oxide synthase. *Diabetes.* 2006;55:496–505.
31. Sun W, Lee TS, Zhu M, Gu C, Wang Y, Zhu Y, Shyy JY. Statins activate AMP-activated protein kinase in vitro and in vivo. *Circulation.* 2006;114:2655–2662.
32. Swan JW, Anker SD, Walton C, Godsland IF, Clark AL, Leyva F, Stevenson JC, Coats AJ. Insulin resistance in chronic heart failure: relation to severity and etiology of heart failure. *J Am Coll Cardiol.* 1997;30:527–532.
33. Nielson C, Lange T. Blood glucose and heart failure in nondiabetic patients. *Diabetes Care.* 2005;28:607–611.
34. Fischer Y, Thomas J, Rosen P, Kammermeier H. Action of metformin on glucose transport and glucose transporter GLUT1 and GLUT4 in heart muscle cells from healthy and diabetic rats. *Endocrinology.* 1995;136:412–420.
35. Russell RR 3rd, Bergeron R, Shulman GI, Young LH. Translocation of myocardial GLUT-4 and increased glucose uptake through activation of AMPK by AICAR. *Am J Physiol.* 1999;277:H643–H649.
36. Davila-Roman VG, Vedala G, Herrero P, de las Fuentes L, Rogers JG, Kelly DP, Gropler RJ. Altered myocardial fatty acid and glucose metabolism in idiopathic dilated cardiomyopathy. *J Am Coll Cardiol.* 2002;40:271–277.
37. Sack MN, Rader TA, Park S, Bastin J, McCune SA, Kelly DP. Fatty acid oxidation enzyme gene expression is downregulated in the failing heart. *Circulation.* 1996;94:2837–2842.
38. Osorio JC, Stanley WC, Linke A, Castellari M, Diep QN, Panchal AR, Hintze TH, Lopaschuk GD, Recchia FA. Impaired myocardial fatty acid oxidation and reduced protein expression of retinoid X receptor-alpha in pacing-induced heart failure. *Circulation.* 2002;106:606–612.
39. Paolisso G, Gambardella A, Galzerano D, D'Amore A, Rubino P, Verza M, Teasuro P, Varricchio M, D'Onofrio F. Total-body and myocardial substrate oxidation in congestive heart failure. *Metabolism.* 1994;43:174–179.
40. Horman S, Beauloye C, Vertommen D, Vanoverschelde JL, Hue L, Rider MH. Myocardial ischemia and increased heart work modulate the phosphorylation state of eukaryotic elongation factor-2. *J Biol Chem.* 2003;278:41970–41976.
41. Inoki K, Zhu T, Guan KL. TSC2 mediates cellular energy response to control cell growth and survival. *Cell.* 2003;115:577–590.
42. Shinbane JS, Wood MA, Jensen DN, Ellenbogen KA, Fitzpatrick AP, Scheinman MM. Tachycardia-induced cardiomyopathy: a review of animal models and clinical studies. *J Am Coll Cardiol.* 1997;29:709–715.
43. Montagnani M, Chen H, Barr VA, Quon MJ. Insulin-stimulated activation of eNOS is independent of Ca^{2+} but requires phosphorylation by Akt at Ser(1179). *J Biol Chem.* 2001;276:30392–30398.
44. Fulton D, Gratton JP, McCabe TJ, Fontana J, Fujio Y, Walsh K, Franke TF, Papapetropoulos A, Sessa WC. Regulation of endothelium-derived nitric oxide production by the protein kinase Akt. *Nature.* 1999;399:597–601.
45. Shiojima I, Walsh K. Regulation of cardiac growth and coronary angiogenesis by the Akt/PKB signaling pathway. *Genes Dev.* 2006;20:3347–3365.

CLINICAL PERSPECTIVE

Metformin is widely used as an antidiabetic drug with an insulin-sensitizing effect. A large-scale clinical trial (the UK Prospective Diabetes Study [UKPDS] 34) has shown that metformin therapy decreased the risk of cardiovascular death and the incidence of myocardial infarction associated with diabetes mellitus; metformin reduced the hemoglobin A_{1c} levels in treated patients to the same extent as in the other patients treated with conventional therapies. These results suggest that metformin might exert cardioprotective effects beyond its glucose-lowering action such as either activation of AMP-activated protein kinase (AMPK) or elevation of nitric oxide. Metformin is known to activate AMPK, which mediates potent cardioprotection against ischemia/reperfusion injury. AMPK also is activated in experimental failing myocardium, suggesting that activation of AMPK is beneficial for the pathophysiology of heart failure. The present study demonstrated that long-term oral administration of metformin prevents the progression of heart failure as indicated by hemodynamic and echocardiographic parameters. Metformin also promoted phosphorylation of both AMPK and endothelial nitric oxide synthase, increased plasma nitric oxide levels, and improved insulin resistance. As a result of these effects, metformin decreased apoptosis and improved cardiac function in failing canine hearts. Interestingly, another AMPK activator (AICAR) had effects equivalent to those of metformin, suggesting the primary role of AMPK activation in reducing apoptosis and preventing heart failure. Drugs that activate AMPK, especially metformin, may provide a novel strategy for the treatment of heart failure in clinical settings.

Journal of the American College of Cardiology
© 2009 by the American College of Cardiology Foundation
Published by Elsevier Inc.

Vol. 53, No. 8, 2009
ISSN 0735-1097/09/$36.00
doi:10.1016/j.jacc.2008.11.014

PRE-CLINICAL RESEARCH

Prolonged Targeting of Ischemic/Reperfused Myocardium by Liposomal Adenosine Augments Cardioprotection in Rats

Hiroyuki Takahama, MD,*†‡ Tetsuo Minamino, MD, PHD,§ Hiroshi Asanuma, MD, PHD,† Masashi Fujita, MD, PHD,§ Tomohiro Asai, PHD,¶ Masakatsu Wakeno, MD, PHD,*†‡ Hideyuki Sasaki, MD,*†‡ Hiroshi Kikuchi, PHD,# Kouichi Hashimoto,** Naoto Oku, PHD,¶ Masanori Asakura, MD, PHD,† Jiyoong Kim, MD,† Seiji Takashima, MD, PHD,§ Kazuo Komamura, MD, PHD,‖ Masaru Sugimachi, MD, PHD,‖ Naoki Mochizuki, MD, PHD,*‡ Masafumi Kitakaze, MD, PHD, FACC†

Osaka, Shizuoka, and Tokyo, Japan

Objectives The purpose of this study was to investigate whether liposomal adenosine has stronger cardioprotective effects and fewer side effects than free adenosine.

Background Liposomes are nanoparticles that can deliver various agents to target tissues and delay degradation of these agents. Liposomes coated with polyethylene glycol (PEG) prolong the residence time of drugs in the blood. Although adenosine reduces the myocardial infarct (MI) size in clinical trials, it also causes hypotension and bradycardia.

Methods We prepared PEGylated liposomal adenosine (mean diameter 134 ± 21 nm) by the hydration method. In rats, we evaluated the myocardial accumulation of liposomes and MI size at 3 h after 30 min of ischemia followed by reperfusion.

Results The electron microscopy and ex vivo bioluminescence imaging showed the specific accumulation of liposomes in ischemic/reperfused myocardium. Investigation of radioisotope-labeled adenosine encapsulated in PEGylated liposomes revealed a prolonged blood residence time. An intravenous infusion of PEGylated liposomal adenosine (450 μg/kg/min) had a weaker effect on blood pressure and heart rate than the corresponding dose of free adenosine. An intravenous infusion of PEGylated liposomal adenosine (450 μg/kg/min) for 10 min from 5 min before the onset of reperfusion significantly reduced MI size (29.5 ± 6.5%) compared with an infusion of saline (53.2 ± 3.5%, $p < 0.05$). The antagonist of adenosine A_1, A_{2a}, A_{2b}, or A_3 subtype receptor blocked cardioprotection observed in the PEGylated liposomal adenosine-treated group.

Conclusions An infusion as PEGylated liposomes augmented the cardioprotective effects of adenosine against ischemia/reperfusion injury and reduced its unfavorable hemodynamic effects. Liposomes are promising for developing new treatments for acute MI. (J Am Coll Cardiol 2009;53:709–17) © 2009 by the American College of Cardiology Foundation

Liposomes are now widely used for drug delivery in cancer treatment to target specific organs actively or passively and to prevent the degradation of chemotherapy agents (1). However, the application of liposomes for cardiovascular diseases is still limited. In ischemic/reperfused myocardium, cellular permeability is enhanced and vascular endothelial integrity is disrupted (2,3), suggesting that nanoparticles

See page 718

*From the Department of Molecular Imaging in Cardiovascular Medicine, Osaka University Graduate School of Medicine, Osaka, Japan; †Department of Cardiovascular Medicine, National Cardiovascular Center, Osaka, Japan; ‡Department of Structural Analysis, Research Institute, National Cardiovascular Center, Osaka, Japan; §Department of Cardiovascular Medicine, Osaka University Graduate School of Medicine, Osaka, Japan; ‖Department of Cardiovascular Dynamics, Research Institute, National Cardiovascular Center, Osaka, Japan; ¶Department of Medical Biochemistry, School of Pharmaceutical Sciences, University of Shizuoka, Shizuoka, Japan; #Daiichi Pharmaceutical Co., Tokyo, Japan; and the **Daiichi-Sankyo Pharmaceutical Co., Tokyo, Japan. Supported by a grant for Scientific Research and a grant for the Advancement of Medical Equipment from the Japanese Ministry of Health, Labor, and Welfare, as well as a grant from the Japan Cardiovascular Research Foundation.

Manuscript received September 4, 2008; revised manuscript received October 21, 2008, accepted November 3, 2008.

JACC Vol. 53, No. 8, 2009
February 24, 2009:709–17

Abbreviations and Acronyms

8-SPT = 8-(p-sulfophenyl) theophylline
EM = electron microscopy
MI = myocardial infarction
PEG = polyethylene glycol
RI = radioisotope
TTC = triphenyltetrazolium chloride

such as liposomes may be a promising drug delivery system for targeting damaged myocardium with cardioprotective agents. Additionally, coating liposomes with polyethylene glycol (PEG) prolongs their residence time in the circulation (1). Because enhanced microvascular permeability persists for at least 48 h after the occurrence of myocardial infarction (MI) (2), drugs delivered in PEGylated liposomes should be able to display their maximum beneficial effects on myocardial damage after MI.

Adenosine has multiple physiological functions that are mediated via the adenosine A_1, A_{2a}, A_{2b}, and A_3 receptors (4,5). Although large-scale clinical trials suggested the potential value of adenosine therapy for patients with acute MI (6,7), this agent has an extremely short half-life (1 to 2 s) and causes hypotension and bradycardia because of vasodilatory and negative chronotropic effects (4). Because a high dose of adenosine is required to exert cardioprotective effects, it is difficult to use clinically because of the associated hemodynamic consequences. Therefore, we hypothesized that adenosine encapsulated in PEGylated liposomes would cause less hemodynamic disturbance and might also specifically accumulate in ischemic/reperfused myocardium, leading to augmented cardioprotective effects. To test this hypothesis, we created PEGylated liposomal adenosine by the hydration method and investigated: 1) whether liposomal adenosine accumulated in ischemic/reperfused myocardium and prolonged blood residence time; 2) whether liposomal adenosine caused less severe hypotension and bradycardia than free adenosine; and 3) which adenosine receptor subtype was involved in mediating the cardioprotective effects of liposomal adenosine against ischemia/reperfusion injury.

Methods

Materials. The materials for preparing PEGylated liposomes, including hydrogenated soy phosphatidyl choline (HSPC), 1,2-distearoyl-sn-glycero-3-phosphoethanolamine-n-[methoxy (polyethylene glycol)-2000] (DSPE-PEG2000), and cholesterol were obtained from Nissei Oil Co., Ltd. (Tokyo, Japan) and Wako Pure Chemical Co., Ltd. (Osaka, Japan). [^{3}H]-adenosine was purchased from Daiichi Pure Chemicals Co., Ltd. (Tokyo, Japan). Other materials were obtained from Sigma (St. Louis, Missouri), including 8-(*p*-sulfophenyl)theophylline (8-SPT; a nonselective adenosine receptor antagonist), 1,3-diethyl-8-phenylxanthine (DPCPX; a selective adenosine A_1 receptor antagonist), 5-amino-7-(phenylethyl)-2-(2-furyl)-pyrazolo[4,3-e]-1,2,4-triazolo[1,5-c] pyrimidine (SCH58261; a selective adenosine A_{2a} receptor antagonist), 8-[4-[((4-cyanophenyl)carbamoylmethyl) oxy]phenyl]-1, 3-di(n-propyl)xanthine (MRS1754; a selective adenosine A_{2b} receptor antagonist), and 5-propyl-2-ethyl-4-propyl-3-(ethylsulfanylcarbonyl)-6-phenylpyridine-5-carboxylate (MRS1523, a selective adenosine A_3 receptor antagonist).

Animals. Male Wistar rats (9 weeks old and weighing 250 to 310 g, Japan Animals, Osaka, Japan) were used. The animal experiments were approved by the National Cardiovascular Center Research Committee and were performed according to institutional guidelines.

Preparation of PEGylated liposomes. The PEGylated liposomes were prepared by the hydration method. Briefly, adenosine was added to the lipid solution. After mixture of lipid and adenosine, DSPE-PEG2000 was added and incubated. The final composition of PEGylated liposomes was HSPC:cholesterol:DSPE-PEG2000 = 6.0:4.0:0.3 (molar ratio). After ultracentrifugation several times, the pellet of liposomal adenosine was resuspended in sodium lactate at each required concentration for use in the experimental protocols. Some samples of final liposomal adenosine were disrupted by dilution with 50% methanol (1.5 ml per 30-μl of liposomes). After 10 min of ultracentrifugation, the concentration of adenosine in the supernatant was measured by high-performance liquid chromatography.

To prepare fluorescent-labeled liposomes, 0.5 mol% tetramethylrhodamine isothiocyanate (rhodamine) was added to the lipid mixture. To prepare radioisotope (RI)-labeled adenosine encapsulated in liposomes, [^{3}H]-radiolabeled adenosine (Daiichi Pure Chemicals, Tokyo, Japan) was diluted with free adenosine and was encapsulated in liposomes as described above.

Characterization of PEGylated liposomal adenosine. The characterization of the liposomes was performed by the dynamic scatter analysis (Zetasizer Nano ZS, Malvern, Worcestershire, United Kingdom). The analyses were performed 10 times per sample, and results represented analyses of 4 independent experiments.

Experimental protocols. PROTOCOL 1: EFFECTS OF PEGYLATED LIPOSOMAL ADENOSINE ON HEMODYNAMICS IN RATS. Rats were anesthetized with intraperitoneal sodium pentobarbital (50 mg/kg). Catheters were advanced into a femoral artery and vein for the measurement of systemic blood pressure and infusion of drugs, respectively. Both blood pressure and heart rate were monitored continuously during the study using a Power Lab (AD Instruments, Castle Hill, Australia). After hemodynamics became stable, we intravenously administered empty PEGylated liposomes (n = 8), free adenosine (n = 8), or PEGylated liposomal adenosine (n = 8) for 10 min. Either PEGylated liposomal or free adenosine was infused at an initial dose of 225 μg/kg/min (0.1 ml/min) for 10 min. After a 5-min interval, either PEGylated liposomal adenosine or free adenosine was infused at 450 μg/kg/min (0.1 ml/min) for 10 min. In the same manner, PEGylated liposomal adenosine or free adenosine was then infused at 900 μg/kg/min (0.1 ml/min).

PROTOCOL 2: EFFECTS OF PEGYLATED LIPOSOMAL ADENOSINE ON INFARCT SIZE IN RATS. The MI was induced by transient ligation of the left coronary artery as described previously (8). In the first series of experiments, to examine the dose-dependent effects of liposomal adenosine on MI size, PEGylated liposomal adenosine was infused intravenously at 50, 150, or 450 μg/kg/min for a 10-min period starting from 5 min before the onset of reperfusion. In the second series of experiments, to determine the adenosine receptor subtype involved in cardioprotective effects by the liposomal adenosine, the antagonist of adenosine subtype receptor was intravenously injected as a bolus followed by the infusion of liposomal adenosine for 10 min. The MI size was evaluated at 3 h after the start of reperfusion. The doses of adenosine receptor subtype antagonists were determined according to the previous reports (9–11).

Measurement of infarct size. At 3 h after the onset of reperfusion, the area at risk and the infarcted area were determined by Evans blue and triphenyltetrazolium chloride (TTC) staining, respectively, as previously described (8). Infarct size was calculated as [infarcted area/area at risk] × 100(%) in a blind manner. The area at risk was composed of border (TTC staining) and infarcted (TTC nonstaining) areas.

Electron microscopy (EM). Myocardial samples for EM were obtained from the central and peripheral areas in ischemic/reperfused myocardium, which roughly corresponded to the infarcted and border areas, respectively, after the left coronary artery was occluded for 30 min of ischemia followed by 3 h of reperfusion. Samples were prepared as previously reported (12). Liposomes, whose major membrane component is unsaturated phospholipids, were visualized as homogenous dark dots with a diameter of 100 to 150 nm (13).

Accumulation of fluorescent-labeled PEGylated liposomes in ischemic/reperfused myocardium. Unlabeled or fluorescent-labeled PEGylated liposomes were infused intravenously at a dose of 0.1 ml/min as liposomal adenosine was infused in protocol 2. At 3 h after reperfusion, hearts were quickly removed and cut into 4 sections parallel to the axis from base to apex. Then ex vivo bioluminescence imaging was performed with an Olympus OV 100 imaging system (Olympus, Tokyo, Japan) and signals were quantified using WASABI quantitative software (Hamamatsu Photonics K.K., Shizuoka, Japan). Fluorescent intensity in the region of interest was measured as previously reported (14). Control intensity indicated the fluorescent intensity in the nonischemic area of the individual rat.

Time-course changes of free and PEGylated liposomal RI-labeled adenosine in plasma and myocardium. Free or PEGylated liposomal [^{3}H]-adenosine (83 kBq per rat) was infused intravenously at a dose of 0.1 ml/min as liposomal adenosine was infused in protocol 2. At the time indicated, rat hearts were harvested for counting of radioactivity (LSC-3100, Aloka Co., Tokyo, Japan). Results are expressed as a percentage of the injected dose per 1 ml of blood or 1 g of wet tissue weight.

Statistical analysis. The parameters of the liposomes were expressed as the average ± SD, whereas other data were expressed as the average ± SEM. Comparison of time-course changes in hemodynamic parameters between groups was performed by 2-way repeated-measures analysis of variance (ANOVA) followed by a post-hoc Bonferroni test. For comparison of RI activity between groups, statistical analysis was done with the Mann-Whitney *U* test. To address the differences in infarct size among groups, we performed a nonparametric (Kruskal-Wallis) test followed by evaluation with the Mann-Whitney *U* test. Resulting p values were corrected according to the Bonferroni method. To compare parameters of liposomes, an unpaired *t* test was performed. In all analyses, $p < 0.05$ was considered to indicate statistical significance.

Results

Characterization of liposomes by dynamic light scatter analysis. The dynamic light scatter analysis showed no significant difference in mean diameter, polydispersity index, or zeta-potential distribution between empty and adenosine-loaded PEGylated liposomes (Table 1).

Liposomes in ischemic/reperfused myocardium. The EM revealed the intact vascular endothelial cells and cardiomyocytes in the nonischemic myocardium (Figs. 1A and 1B). There were no homogenous dark dots indicating liposomes in the nonischemic myocardium of rats that received either saline (Fig. 1A) or liposomes (Fig. 1B). In the border area, many homogenous dark dots indicating liposomes were accumulated in rats that received liposomes, but not saline (Figs. 1C and 1D). In this area, significant structural damage was not observed in endothelium, but slight swelling of mitochondria was often observed. In the infarcted area, numerous liposomes were detected in rats that received liposomes, but not saline (Figs. 1E and 1F). In this area, the disrupted endothelial integrity and marked swelling of mitochondria were often observed.

Table 1 Characterization of Liposomes by Dynamic Light Scatter Analysis

	Mean Diameter (nm)	Polydispersity Index	Zeta Potential (mV)
PEGylated liposomes (empty liposomes)	126 ± 12	0.035 ± 0.003	−1.7 ± 0.4
PEGylated liposomal adenosine	134 ± 21	0.094 ± 0.002	−2.3 ± 1.1

Results represented analysis of 4 independent experiments. Values are expressed as mean ± SD.
PEG = polyethylene glycol.

JACC Vol. 53, No. 8, 2009
February 24, 2009:709–17

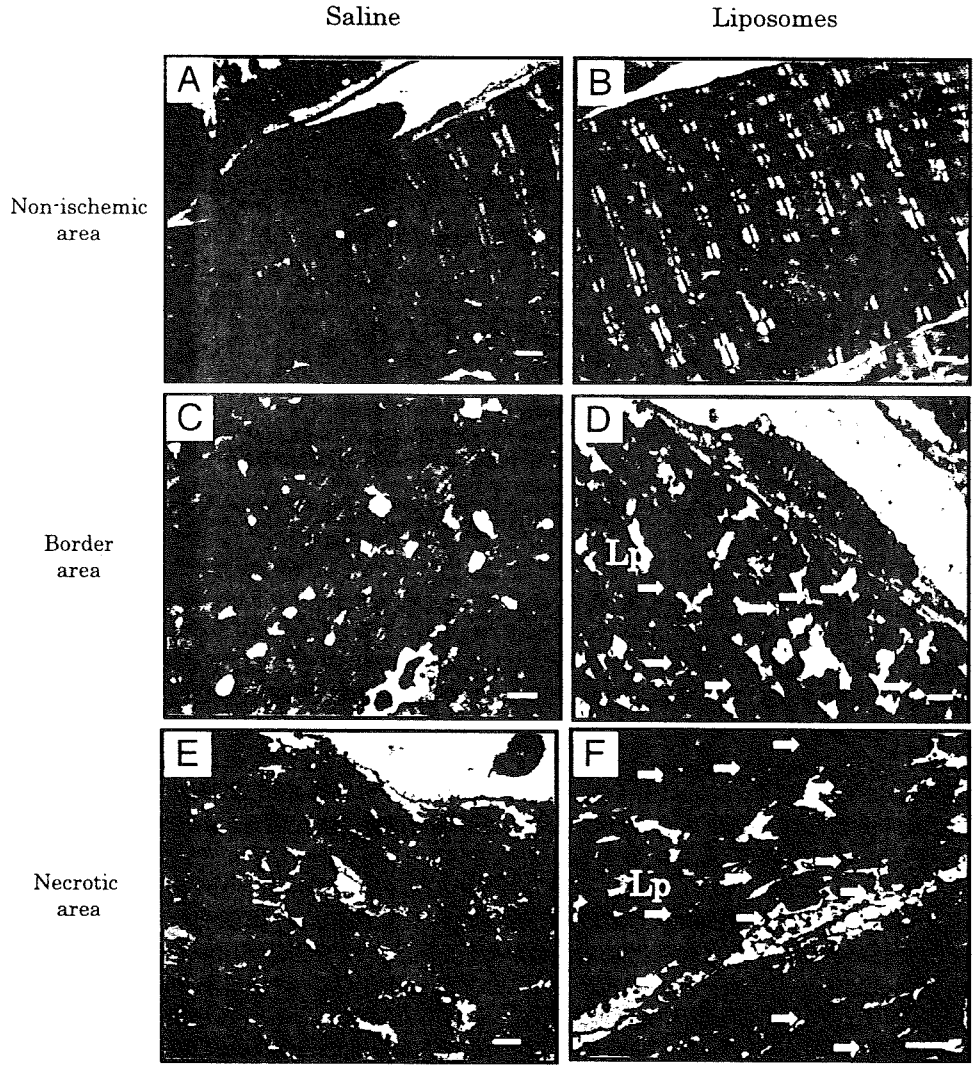

Figure 1 **Liposomes in Ischemic/Reperfused Myocardium**

(A, B) Representative electron micrographs of the nonischemic area in rats that received saline **(A)** or liposomes (Lp) **(B)**. **(C, D)** Representative electron micrographs of border area at 3 h after myocardial infarction (MI). Many **dark dots** accumulated in this area in the rat that received liposomes but not saline. **(E, F)** Representative electron micrographs of infarcted areas at 3 h after MI. Numerous **dark dots** accumulated in this area in the rat that received liposomes but not saline. Scale bars represent 1 μm.

Fluorescent-labeled PEGylated liposomes in ischemic/reperfused myocardium. Quantitative analysis by bioluminescence ex vivo bioluminescene imaging revealed that the target to control fluorescent intensity ratio was higher in the border (noninfarcted area at risk) as well as infarcted areas compared with a nonischemic one, suggesting that fluorescent-labeled liposomes were accumulated in the border as well as infarcted areas. Since there was no high-intensity area when unlabeled liposomes were infused, it was suggested that this was not a nonspecific phenomenon to MI by the ex vivo bioluminescence imaging system (Fig. 2). The Evans blue staining was unrelated to the fluorescence intensity (data not shown).

Plasma radioactivity of RI-labeled adenosine was markedly higher in the PEGylated liposomal adenosine group at 10 min and 3 h after the intravenous infusion than in the free adenosine group (Fig. 3A). Encapsulation within PEGylated liposomes also augmented the accumulation of adenosine in ischemic/reperfused myocardium compared with that of free adenosine (Fig. 3B).

Hemodynamic effects of PEGylated liposomal adenosine. Baseline hemodynamic parameters did not differ among the groups. An intravenous infusion of free adenosine at doses of 225, 450, and 900 μg/kg/min decreased the mean blood pressure by 14.8%, 25.4%, and 33.7%, respectively, compared with the effect of empty PEGylated lipo-

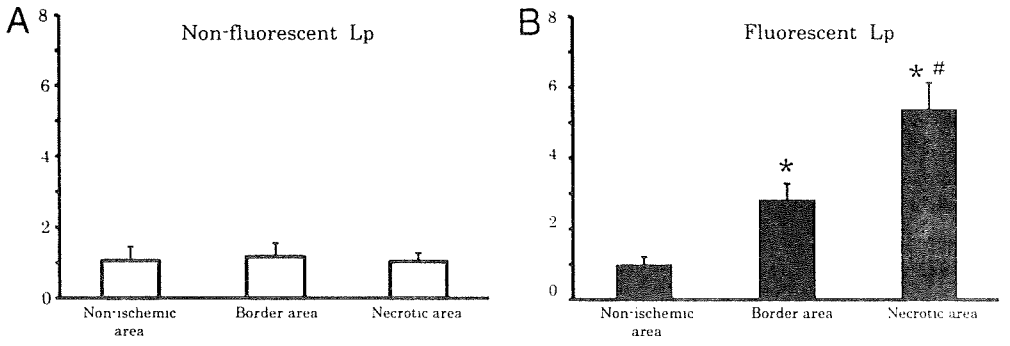

Figure 2 **Detection of Fluorescence-Labeled PEGylated Liposomes in Ischemic/Reperfused Myocardium**

Quantitative analysis of target-to-control fluorescent intensity ratio for each area in rats (n = 3 each group) that received nonfluorescent **(A)** or fluorescent **(B)** liposomes. The values of bioluminescence signals in the border and infarcted areas were expressed as the fold to that of the each nonischemic area. Values are expressed as the mean ± SEM (error bars). *p < 0.05 versus nonischemic areas. #p < 0.05 versus border areas.

somes. In contrast, the intravenous infusion of PEGylated liposomal adenosine at a dose of either 225 or 450 μg/kg/min did not significantly alter mean blood pressure (Fig. 4). Changes of the heart rate after infusion of PEGylated liposomal adenosine or free adenosine were similar to those observed for mean blood pressure (Fig. 4).

Effects of PEGylated liposomal adenosine on MI size. Baseline hemodynamic parameters were similar among all of the groups (Table 2). Intravenous infusion of free adenosine for 10 min reduced both the blood pressure and the heart rate, although these parameters returned to baseline within 5 min of ceasing infusion (Table 2). In contrast, hemodynamic parameters of the other groups were not altered (Table 2). The area at risk in the control group (61 ± 3%) did not differ compared with those of other groups that received liposomal adenosine. Intravenous infusion of PEGylated liposomal adenosine caused a dose-dependent decrease of MI size compared with that in the control group, whereas intravenous infusion of empty PEGylated liposomes or free adenosine did not (Fig. 5B).

The bolus injection of adenosine receptor antagonist did not alter the hemodynamic parameters (Table 3). The area at risk in the liposomal adenosine group (58 ± 3%) did not differ compared with those of other groups that received adenosine receptor antagonist. Infusion of 8-SPT, a nonspecific adenosine receptor antagonist, blunted the cardioprotective effect of liposomal adenosine (Fig. 6B). Furthermore, the infusion of the adenosine A_1, A_{2a}, A_{2b}, or A_3 receptor antagonist also blunted cardioprotective effects of liposomal adenosine (Fig. 6B). Infusion of 8-SPT alone did not significantly affect myocardial infarct size compared with the control (52 ± 5%, n = 4).

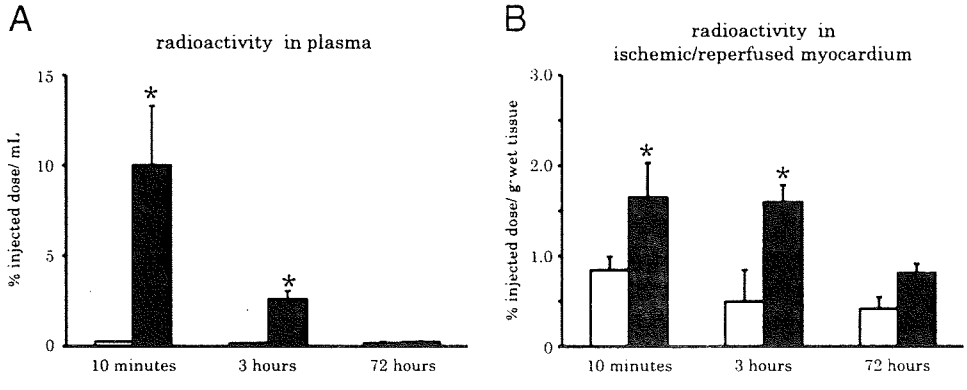

Figure 3 **Radioisotope-Labeled Adenosine in Plasma and Ischemic/Reperfused Myocardium**

(A) Changes in plasma radioactivity after infusion of radioisotope-labeled adenosine. **Solid and open bars** indicate the PEGylated liposomal adenosine and free adenosine groups, respectively (n = 4 each). In the PEGylated liposomal adenosine group, plasma radioactivity was markedly higher than in the free adenosine group. **(B)** Changes in radioactivity in ischemic/reperfused myocardium. **Solid and open bars** indicate the PEGylated liposomal adenosine and free adenosine groups, respectively (n = 4 each). In the PEGylated liposomal adenosine group, myocardial radioactivity was markedly higher than in the free adenosine group. Values are expressed as the mean ± SEM (error bars). *p < 0.05 versus the free adenosine group at the corresponding time.

JACC Vol. 53, No. 8, 2009
February 24, 2009:709–17

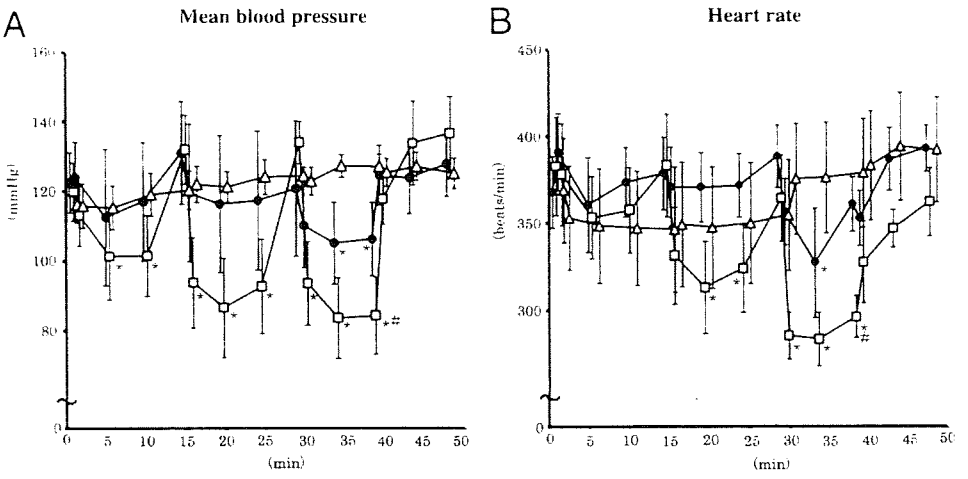

Figure 4 **Hemodynamic Effects of PEGylated Liposomal Adenosine**

Changes in the mean blood pressure **(A)** and heart rate **(B)** after intravenous infusion of various doses of empty PEGylated liposomes **(triangles)**, PEGylated liposomal adenosine **(circles)**, or free adenosine **(squares)** (n = 8 each). Values are expressed as the mean ± SEM. *p < 0.05 versus baseline at the corresponding group. #p < 0.05 versus PEGylated liposomes.

Discussion

In the present study, EM, bioluminescence ex vivo imaging, and fluorescent analysis revealed the accumulation of liposomes in the border (noninfarcted areas at risk) as well as infarcted ones, but not nonischemic myocardium, at 3 h after MI. These findings suggested that liposomes could specifically accumulate in ischemic/reperfused myocardium. Interestingly, EM revealed the existence of liposomes at sites where endothelial integrity was still morphologically maintained. Endothelial dysfunction such as enhanced permeability is induced by ischemic insult without morphological endothelial disruption (3,15). Enhanced permeability might lead to the accumulation of liposomes in the border as well as infarcted area, which will contribute to salvage the ischemic/reperfused myocardium. However, further investigation will be needed to determine the precise mechanism by which liposomes accumulate in ischemic/reperfused myocardium.

Analysis using RI-labeled adenosine encapsulated in liposomes revealed that plasma radioactivity was markedly higher in the PEGylated liposomal adenosine group compared with the free adenosine group. This indicates that encapsulation of adenosine by PEGylated liposomes considerably prolonged its residence time in the circulation and delayed its degradation. Consistent with the histological data, RI-labeled adenosine also showed preferential accumulation in ischemic/reperfused myocardium.

Table 2 **Effects of Liposomal Adenosine on Hemodynamic Parameters**

		Ischemia				Reperfusion	
	Baseline	0 min	15 min	25 min	30 min	5 min	10 min
Mean blood pressure (mm Hg)							
Saline	122 ± 5	102 ± 10	108 ± 7	107 ± 9	108 ± 7	105 ± 9	104 ± 9
Vehicle	127 ± 4	109 ± 8	108 ± 7	111 ± 9	111 ± 5	105 ± 5	103 ± 5
Free-Ado	124 ± 8	115 ± 8	111 ± 5	109 ± 4	66 ± 4*	62 ± 4*	112 ± 6
Lp-Ado 50 μg/kg/min	121 ± 5	106 ± 6	105 ± 6	110 ± 10	102 ± 6	101 ± 6	104 ± 4
Lp-Ado 150 μg/kg/min	122 ± 3	107 ± 6	107 ± 6	109 ± 11	105 ± 6	100 ± 6	103 ± 4
Lp-Ado 450 μg/kg/min	124 ± 3	104 ± 6	105 ± 6	107 ± 5	102 ± 6	99 ± 6	104 ± 4
Heart rate (beats/min)							
Saline	363 ± 22	366 ± 19	369 ± 14	413 ± 22	372 ± 12	372 ± 16	371 ± 14
Vehicle	363 ± 32	363 ± 6	383 ± 6	396 ± 25	367 ± 6	374 ± 7	372 ± 7
Free-Ado	360 ± 18	361 ± 17	384 ± 13	379 ± 18	305 ± 11*	293 ± 13*	356 ± 14
Lp-Ado 50 μg/kg/min	378 ± 19	386 ± 21	366 ± 12	376 ± 12	367 ± 19	369 ± 9	377 ± 17
Lp-Ado 150 μg/kg/min	388 ± 27	376 ± 20	371 ± 14	377 ± 13	378 ± 16	373 ± 16	369 ± 17
Lp-Ado 450 μg/kg/min	368 ± 17	376 ± 21	361 ± 13	386 ± 15	368 ± 15	363 ± 6	367 ± 7

Values are expressed as mean ± SEM. *p < 0.05 versus baseline.
Free-Ado = free adenosine; Lp-Ado = PEGylated liposomal adenosine; PEG = polyethylene glycol; vehicle = PEGylated liposomes.

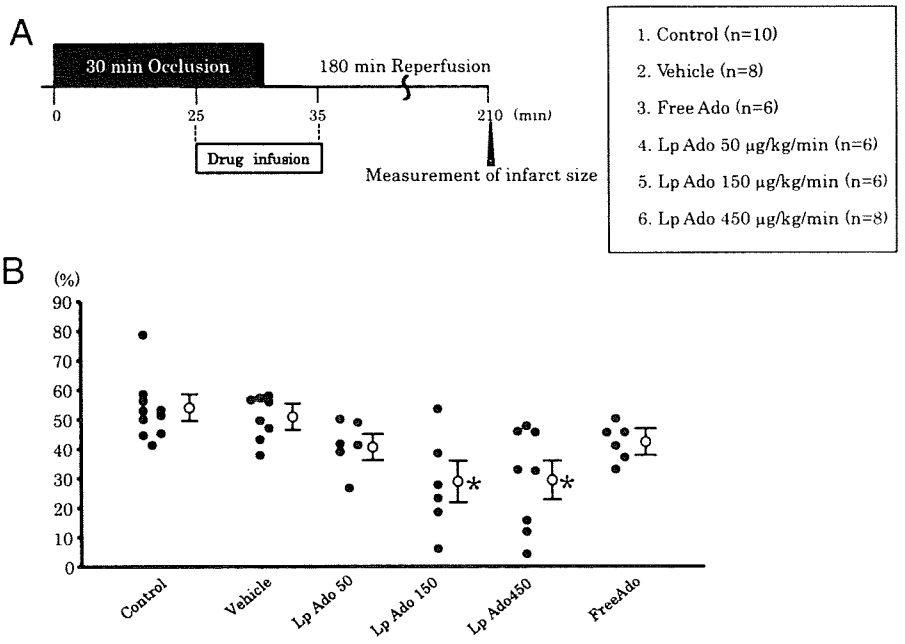

Figure 5 **Dose-Dependent Effects of PEGylated Liposomal Adenosine on Myocardial Infarct Size**

(A) Protocol showing the timing of infusion of PEGylated liposomal adenosine and of infarct size measurement. **(B)** Myocardial infarct size. Values are expressed as mean ± SEM (error bars). *$p < 0.05$ versus the control group. Free-Ado = free adenosine; Lp-Ado = PEGylated liposomal adenosine; Vehicle = PEGylated liposomes.

Furthermore, this study showed that PEGylated liposomal adenosine had a weaker effect on the blood pressure and heart rate than free adenosine. Thus, encapsulating adenosine in PEGylated liposomes attenuated its vasodilatory and negative chronotropic effects, presumably by reducing the amount of circulating free adenosine. However, the changes of hemodynamic parameters in this in vivo model suggested that significant release of adenosine from PEGylated liposomes would still occur if a large dose of liposomal adenosine (e.g., 900 μg/kg/min) were administered. Thus, further investigation of the in vivo pharmacodynamics of PEGylated liposomal adenosine is needed.

An intravenous infusion of PEGylated liposomal adenosine at the maximum dose that did not disturb hemodynamic parameters for 10 min before reperfusion reduced MI size in a dose-dependent manner, and this improvement was blocked by 8-SPT, a nonselective adenosine receptor antagonist. These findings suggest that adenosine released from liposomes acts via an adenosine receptor-dependent pathway. One possible mechanism by which PEGylated lipo-

Table 3 **Effects of Adenosine Receptor Antagonist on Hemodynamic Parameters**

		Ischemia				Reperfusion	
	Baseline	0 min	15 min	25 min	30 min	5 min	10 min
Mean blood pressure (mm Hg)							
Lp-Ado + 8SPT	120 ± 6	113 ± 4	112 ± 6	112 ± 5	107 ± 6	102 ± 8	109 ± 7
Lp-Ado + DPCPX	130 ± 6	105 ± 4	121 ± 4	100 ± 10	122 ± 6	120 ± 6	111 ± 4
Lp-Ado + SCH58261	132 ± 2	98 ± 12	99 ± 8	110 ± 8	118 ± 10	113 ± 10	109 ± 6
Lp-Ado + MRS1754	130 ± 3	95 ± 12	106 ± 8	105 ± 10	100 ± 10	96 ± 10	99 ± 7
Lp-Ado + MRS1523	130 ± 2	109 ± 8	104 ± 8	105 ± 9	100 ± 9	101 ± 10	104 ± 6
Heart rate (beats/min)							
Lp-Ado + 8SPT	404 ± 17	385 ± 10	374 ± 8	396 ± 8	389 ± 9	383 ± 8	385 ± 9
Lp-Ado + DPCPX	396 ± 24	380 ± 11	399 ± 9	398 ± 12	385 ± 9	382 ± 9	380 ± 7
Lp-Ado + SCH58261	393 ± 14	399 ± 15	381 ± 9	395 ± 15	376 ± 9	373 ± 9	385 ± 7
Lp-Ado + MRS1754	398 ± 14	392 ± 11	401 ± 9	379 ± 15	378 ± 9	374 ± 9	377 ± 7
Lp-Ado + MRS1523	396 ± 9	390 ± 11	390 ± 11	392 ± 10	373 ± 9	391 ± 7	388 ± 11

Values were expressed as mean ± SEM. *$p < 0.05$ versus baseline.
Lp-Ado = PEGylated liposomal adenosine; PEG = polyethylene glycol; Vehicle = PEGylated liposomes.

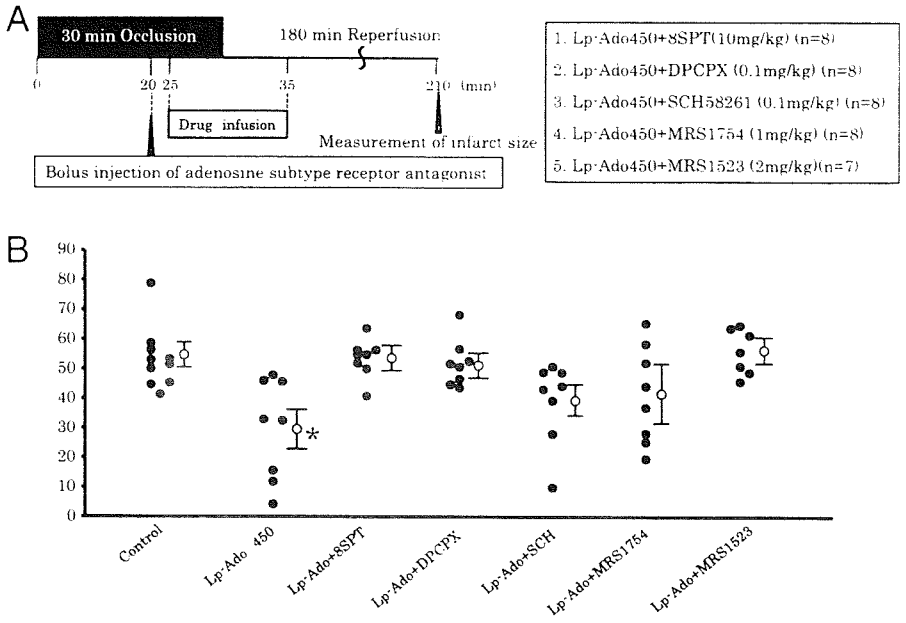

Figure 6 **Effects of Adenosine Receptor Antagonists on Myocardial Infarct Size**

(A) Protocol showing the timing of infusion of PEGylated liposomal adenosine and bolus injection adenosine receptor antagonists. **(B)** Myocardial infarct size. Values are expressed as the mean ± SEM (error bars). *$p < 0.05$ versus the control group. The abbreviations for adenosine antagonists were described in the text. Abbreviations as in Figure 5.

somes could augment cardioprotective effects of liposomal adenosine with minimum effects on hemodynamic parameters is the enhanced accumulation of PEGylated liposomal adenosine in ischemic/reperfused myocardium, which could augment various beneficial actions such as preventing calcium overload in the myocardium (5). The prolonged persistence of PEGylated liposomal adenosine would also increase its beneficial effect on ischemic/reperfused myocardium. Although continuous high-dose, long-term infusion of free adenosine was reported to reduce infarct size in rats (16), the present study did not confirm such a cardioprotective effect, probably because the total dose of free adenosine that we used was not high enough.

We found that myocardial infarct size in the group that received PEGylated liposomal adenosine with the antagonist of adenosine A_1, A_{2a}, A_{2b}, or A_3 subtype receptor was no different from the control group, indicating that every adenosine subtype receptor could possibly play a role in mediating cardioprotection by liposomal adenosine and that it was difficult to identify one particular subtype in the present study. Numerous studies reported that A_1, A_{2a}, A_{2b}, and A_3 receptors have been involved in cardioprotection against ischemia/reperfusion injury, and it remains controversial which adenosine subtype receptor is most responsible for cardioprotection (17–20). Furthermore, because the adenosine receptor antagonists used in the present study had some nonspecific effects, future investigation will be needed to examine the precise role of each adenosine receptor subtype using genetically engineered mice.

Because liposomal adenosine infused during reperfusion could reduce MI size, this agent could be a candidate for the adjunctive therapy of patients with acute MI. Importantly, adenosine is currently used for the diagnosis of ischemic heart disease and PEGylated liposomes are used to deliver anticancer agents (21). Thus, it should not be difficult to introduce PEGylated liposomal adenosine into clinical practice. Finally, PEGylated liposomes may provide a useful drug delivery system for targeting ischemic/reperfused myocardium with other agents.

Acknowledgments

The authors thank Akiko Ogai and Yoko Nakano for their excellent technical assistance; Motohide Takahama, Hiroyuki Hao, and Hatsue Ishibashi-Ueda for advice about the electron microscopy figure; and Syunichi Kuroda and Takashi Matsuzaki for assistance with bioluminescence imaging.

Reprint requests and correspondence: Dr. Tetsuo Minamino, Department of Cardiovascular Medicine, Osaka University Graduate School of Medicine, 2-2 Yamadaoka, Suita, Osaka 565-0871, Japan. E-mail: minamino@medone.med.osaka-u.ac.jp.

REFERENCES

1. Papahadjopoulos D, Allen TM, Gabizon A, et al. Sterically stabilized liposomes: improvements in pharmacokinetics and antitumor therapeutic efficacy. Proc Natl Acad Sci U S A 1991;24:11460–4.

2. Horwitz LD, Kaufman D, Keller MW, Kong Y. Time course of coronary endothelial healing after injury due to ischemia and reperfusion. Circulation 1994;90:2439–47.
3. Dauber IM, Van Benthuysen KM, McMurtry IF, et al. Functional coronary microvascular injury evident as increased permeability due to brief ischemia and reperfusion. Circ Res 1990;66:986–98.
4. Forman MB, Stone GW, Jackson EK. Role of adenosine as adjunctive therapy in acute myocardial infarction. Cardiovasc Drug Rev 2006;24:116–47.
5. Mubagwa K, Flameng W. Adenosine, adenosine receptors and myocardial protection: an updated overview. Cardiovasc Res 2001;52:25–39.
6. Mahaffey KW, Pume JA, Barbagelata NA, et al. Adenosine as an adjunct to thrombolytic therapy for acute myocardial infarction: results of a multicenter, randomized, placebo-controlled trial: the Acute Myocardial Infarction STudy of ADenosine (AMISTAD) trial. J Am Coll Cardiol 1999;34:1711–20.
7. Ross AM, Gibbons RJ, Stone GW, Kloner RA, Alexander RW, for the AMISTAD-II ÁInvestigators. A randomized, double-blinded, placebo-controlled multicenter trial of adenosine as an adjunct to reperfusion in the treatment of acute myocardial infarction (AMISTAD-II). J Am Coll Cardiol 2005;45:1775–80.
8. Bullard AJ, Govewalla P, Yellon DM. Erythropoietin protects the myocardium against reperfusion injury in vitro and in vivo. Basic Res Cardiol 2005;100:397–403.
9. Hannon JP, Tigani B, Wolber C, et al. Evidence for an atypical receptor mediating the augmented bronchoconstrictor response to adenosine induced by allergen challenge in activity sensitized Brown Norway rats. Br J Pharmacol 2002;135:685–96.
10. Kin H, Zatta AJ, Lofye MT, et al. Postconditioning reduces infarct size via adenosine receptor activation by endogenous adenosine. Cardiovasc Res 2005;67:124–33.
11. Hinschen AK, RoseMeyer RB, Headrick JP. Adenosine receptor subtypes mediating coronary vasodilation in rat hearts. J Cardiovasc Pharmacol 2003;41:73–80.
12. Kaeffeer N, Richard V, Francois A, Lallemand F, Henry JP, Thuillez C. Preconditioning prevents chronic reperfusion-induced coronary endothelial dysfunction in rats. Am J Physiol 1996;271:H842–9.
13. M Shimizu, Miwa K, Hashimoto Y, Goto A. Encapsulating of chicken egg yolk immunoglobulin G (IgY) by liposomes. Biosci Biotechnol Biochem 1993;57:1445–9.
14. Kasuya T, Jung J, Kadova H, et al. In vivo delivery of bionanocapsules displaying phaseolus vulgaris agglutinin-L(4) isolectin to malignant tumors overexpressing N-acetylglucosaminlyltransferase V. Hum Gene Ther 2008;19:887–95.
15. Kim YD, Fomsgaard JS, Heim KF, et al. Brief ischemia-reperfusion induces stunning of endothelium in canine coronary artery. Circulation 1992;85:1473–82.
16. Canyon SJ, Dobson GP. Protection against ventricular arrhythmias and cardiac death using adenosine and lidocaine during regional ischemia in the in vivo rat. Am J Physiol Heart Circ Physiol 2004;287:H1286–95.
17. Yaar R, Jones MR, Chen JF, Ravid K. Animal models for the study of adenosineÅreceptor function. J Cell Physiol 2005;202:9–20.
18. Norton ED, Jackson EK, Turner MB, Virmani R, Forman MB. The effects of intravenous infusions of selective adenosine A_1-receptor and A_2-receptor agonists on myocardial reperfusion injury. Am Heart J 1992;123:332–8.
19. Xu Z, Mueller RA, Park SS, Boysen PG, Cohen MV, Downey JM. Cardioprotection with adenosine A_2 receptor activation at reperfusion. J Cardiovasc Pharmacol 2005;46:794–802.
20. Vinten-Johansen J. Postconditioning: a mechanical maneuver that triggers biological and molecular cardioprotective responses to reperfusion. Heart Fail Rev 2007;12:235–344.
21. Lasic DD. Doxorubicin in sterically stabilized liposomes. Nature 1996;380:561–2.

Key Words: myocardial infarction ▪ liposome ▪ drug delivery system ▪ adenosine.

PDK1 coordinates survival pathways and β-adrenergic response in the heart

Kaoru Ito[a], Hiroshi Akazawa[a], Masaji Tamagawa[b], Kensuke Furukawa[c], Wataru Ogawa[c], Noritaka Yasuda[a], Yoko Kudo[a], Chien-hui Liao[a], Rie Yamamoto[a], Toshiaki Sato[b], Jeffery D. Molkentin[d], Masato Kasuga[c], Tetsuo Noda[e], Haruaki Nakaya[b], and Issei Komuro[a,1]

Departments of [a]Cardiovascular Science and Medicine and [b]Pharmacology, Chiba University Graduate School of Medicine, 1-8-1 Inohana, Chuo-ku, Chiba 260-8670, Japan; [c]Division of Diabetes, Metabolism, and Endocrinology, Department of Internal Medicine, Kobe University Graduate School of Medicine, 7-5-1 Kusunoki-cho, Chuo-ku, Kobe 650-0017, Japan; [d]Department of Pediatrics, University of Cincinnati, Children's Hospital Medical Center, 3333 Burnet Avenue, Cincinnati, OH 45229; and [e]Department of Cell Biology, Japanese Foundation for Cancer Research, Cancer Institute, 3-10-6 Ariake, Koto-ku, Tokyo 135-8550, Japan

Edited by Eric N. Olson, University of Texas Southwestern Medical Center, Dallas, TX, and approved April 2, 2009 (received for review January 5, 2009)

The 3-phosphoinositide-dependent kinase-1 (PDK1) plays an important role in the regulation of cellular responses in multiple organs by mediating the phosphoinositide 3-kinase (PI3-K) signaling pathway through activating AGC kinases. Here we defined the role of PDK1 in controlling cardiac homeostasis. Cardiac expression of PDK1 was significantly decreased in murine models of heart failure. Tamoxifen-inducible and heart-specific disruption of *Pdk1* in adult mice caused severe and lethal heart failure, which was associated with apoptotic death of cardiomyocytes and β_1-adrenergic receptor (AR) down-regulation. Overexpression of Bcl-2 protein prevented cardiomyocyte apoptosis and improved cardiac function. In addition, PDK1-deficient hearts showed enhanced activity of PI3-Kγ, leading to robust β_1-AR internalization by forming complex with β-AR kinase 1 (βARK1). Interference of βARK1/PI3-Kγ complex formation by transgenic overexpression of phosphoinositide kinase domain normalized β_1-AR trafficking and improved cardiac function. Taken together, these results suggest that PDK1 plays a critical role in cardiac homeostasis in vivo by serving as a dual effector for cell survival and β-adrenergic response.

AGC kinase | apoptosis | heart failure | receptor internalization

Heart failure, a major cause of morbidity and mortality worldwide, is a clinical syndrome in which the heart is incapable of pumping blood at a rate commensurate with systemic demands (1). Injurious stresses from extrinsic or intrinsic origins trigger the complex intracellular signaling pathways in cardiomyocytes and thereby activate the compensatory mechanisms involving alterations in survival and growth signals, calcium handling, and energy production (2). Simultaneously, the sympathetic nervous, renin-angiotensin-aldosterone, and cytokine systems are activated to cope with a decline in cardiac performance. Although these compensatory systems initially maintain cardiac function within a physiological range, prolonged activation of these systems paradoxically leads to cardiac damage and worsens clinical prognosis (2). Therefore, for the elucidation of the pathophysiology of heart failure, it is very important to dissect the inherent complexity of intracellular signaling pathways that coordinate the cellular homeostasis and neurohumoral responses in cardiomyocytes.

The 3-phosphoinositide-dependent protein kinase-1 (PDK1) is a member of the AGC serine/threonine kinase family that functions downstream of phosphoinositide 3-kinase (PI3-K) and activates several AGC kinases, including Akt, p70 ribosomal S6 kinase (p70S6K), and serum- and glucocorticoid-induced protein kinase 1 (SGK1), by phosphorylating these enzymes at their activation loops (3). The physiological functions of PDK1 have been investigated by targeted disruption of *Pdk1* gene. Mouse embryos systemically deficient for *Pdk1* were lethal during early embryogenesis, displaying multiple abnormalities that included lack of somites, forebrain, and neural crest-derived tissues (4). Alessi et al. (5) recently generated striated muscle-specific PDK1 conditional knockout mice (PDK1-MCKCre) by crossing mice harboring a "floxed" *Pdk1* allele with transgenic mice expressing Cre recombinase under the control of the *muscle creatine kinase* (*MCK*) promotor. PDK1-MCKCre mice died of heart failure by 11 weeks of age. Interestingly, PDK1-MCKCre mice showed attenuation of cardimyocyte cell growth and impairment of left ventricular (LV) contraction. It was reported that cardiomyocytes deficient for *Pdk1* were sensitive to hypoxia (5), and that ischemic preconditioning failed to protect *Pdk1*-hypomorphic mutant mice against myocardial infarction (MI) (6). However, the mechanisms of how PDK1 deficiency induces these cardiac abnormalities remain to be resolved.

In this study, we found that the expression levels of PDK1 protein were significantly decreased in the failing hearts of murine models. We generated tamoxifen-inducible and heart-specific PDK1 conditional knockout mice (PDK1-MerCre) to elucidate the relevance of PDK1 to the pathogenesis of heart failure. We disrupted the *Pdk1* gene in the adulthood and demonstrated that PDK1 plays a role in the regulation of normal cardiac function by preventing cardiomyocyte apoptosis and by preserving responsiveness to β-adrenergic stimulation.

Results

Generation of Tamoxifen-Inducible and Heart-Specific PDK1 Knockout Mice. We examined alterations in the expression levels of PDK1 in failing hearts. Heart failure was induced in mice by producing myocardial infarction or administering doxorubicin i.p. Two weeks after operation of myocardial infarction or doxorubicin injection, expression levels of PDK1 were significantly decreased in the failing hearts, compared with control hearts (Fig. S1).

To assess the pathophysiological significance of PDK1 down-regulation, we created a model of temporally regulated inactivation of *Pdk1* specifically in the adult hearts. We crossed $Pdk1^{flox/flox}$ mice (7, 8) with transgenic mice expressing tamoxifen-inducible Cre recombinase protein fused to two mutant estrogen-receptor ligand-binding domains (MerCreMer) under the control of the *α-myosin heavy chain* promoter (9). In the resulting $Pdk1^{flox/flox}$/*MerCreMer*$^{+}$ mice (PDK1-MerCre) at the age of 10 weeks, we administered tamoxifen successively for 5 days and confirmed by immunoblot analysis that functional PDK1 expression was almost undetectable specifically in the hearts on day 7 after the initiation of tamoxifen treatment (Fig. S2*A*).

Next, we examined whether the activation of kinases downstream of PDK1 were suppressed in the hearts of PDK1-MerCre. In

Author contributions: H.A. and I.K. designed research; K.I., M.T., K.F., N.Y., Y.K., C.-h.L., and R.Y. performed research; K.F., J.D.M., and T.N. contributed new reagents/analytic tools; K.I., M.T., W.O., T.S., M.K., and H.N. analyzed data; and K.I., H.A., and I.K. wrote the paper.

The authors declare no conflict of interest.

This article is a PNAS Direct Submission.

[1]To whom correspondence should be addressed. E-mail: komuro-tky@umin.ac.jp.

This article contains supporting information online at www.pnas.org/cgi/content/full/0900064106/DCSupplemental.

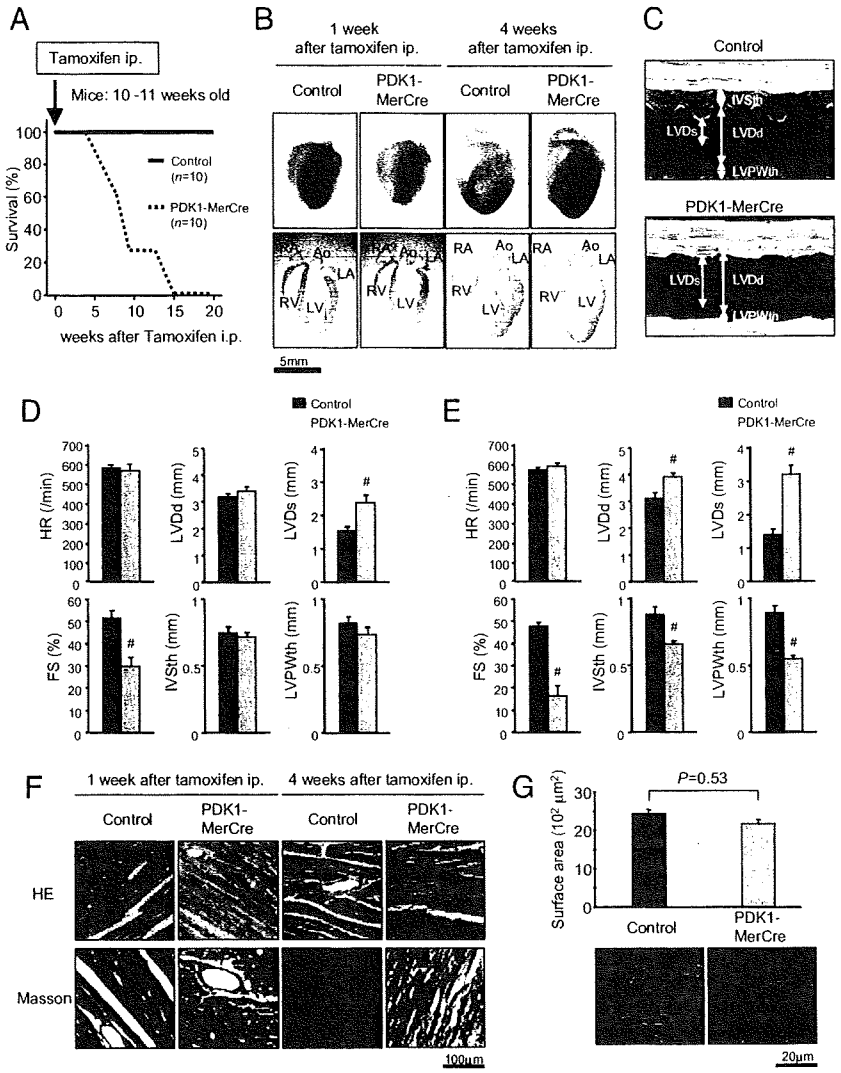

Fig. 1. Severe heart failure observed in PDK1-MerCre mice. (*A*) Kaplan-Meier survival curves of PDK1-MerCre mice (n = 10) and control mice (n = 10). Mice were injected with tamoxifen at the age of 10–11 weeks. (*B*) Macroscopic findings and 4-chamber sections of the hearts from PDK1-MerCre and control mice 1 and 4 weeks after the initiation of tamoxifen treatment. Ao, aorta; LA, left atrium; LV, left ventricule; RA, right atrium; RV, right ventricule. (*C*) Representative M-mode echocardiograms of mice 1 week after tamoxifen treatment. (*D*) Echocardiographic measurements of PDK1-MerCre and control mice 1 week after tamoxifen treatment. HR, heart rate; LVDd, LV dimension in diastole; LVDs, LV dimension in systole; FS, fractional shortening; IVSth, interventricular septum thickness; LVPWth, LV posterior wall thickness. Values represent the mean ± SEM of data from 10 mice in each group. #, $P < 0.01$ versus control group. (*E*) Echocardiographic measurements of PDK1-MerCre and control mice 4 weeks after tamoxifen treatment. Values represent the mean ± SEM of data from 6 mice in each group. #, $P < 0.01$ versus control group. (*F*) Histological sections with hematoxylin and eosin (HE) staining and Masson's trichrome (Masson) staining of PDK1-MerCre and control mice 1 and 4 weeks after tamoxifen treatment. (*G*) Surface areas of isolated cardiomyocytes (57 individual cardiomyocytes in each group) and sample pictures of isolated cardiomyocytes from PDK1-MerCre and control mice 1 week after tamoxifen treatment. Values represent the mean ± SEM.

mammalian cells, Akt is fully activated through PDK1-dependent phosphorylation of Thr-308 and PDK1-independent phosphorylation of Ser-473 (10). Insulin-induced phosphorylation of Akt at Thr-308 in PDK1-MerCre hearts was significantly attenuated, compared with control hearts, while phosphorylation level at Ser-473 was unchanged (Fig. S2*B*). As a consequence, Akt kinase activity was markedly reduced in PDK1-MerCre hearts (Fig. S2*C*). Consistently, insulin-induced phosphorylation levels of glycogen synthase kinase (GSK) 3β at Ser-9, mammalian target of rapamycin (mTOR) at Ser-2448, and p70S6K at Thr-389 (11) were attenuated in the PDK1-MerCre hearts (Fig. S2*B*). Collectively, these results indicate that Akt signaling is inhibited in PDK1-MerCre hearts.

Lethal Heart Failure in PDK1-MerCre Mice. Without tamoxifen treatment, PDK1-MerCre mice survived normally and were indistinguishable in appearance from control littermates. Strikingly, all PDK1-MerCre mice died from 5 to 15 weeks after the initiation of tamoxifen treatment (Fig. 1*A*).

One week after tamoxifen treatment, cardiac sizes were not significantly different between PDK1-MerCre mice and control mice (Fig. 1*B*). Echocardiographic examination revealed a significant decrease in the percent of fractional shortening (%FS), a parameter for contractile function, as early as 1 week after tamoxifen treatment in PDK1-MerCre mice (Fig. 1 *C* and *D*). During this period, there was no increase in LV dimension or thinning of LV wall, which was consistent with the macroscopic findings (Fig. 1 *B* and *D*). However, 4 weeks after tamoxifen treatment, progression of contractile dysfunction together with global chamber dilatation and wall thinning was observed in PDK1-MerCre mice (Fig. 1 *B* and *E*). Histologically, interstitial fibrosis was increased at 1 week in

PDK1-MerCre hearts and further enhanced at 4 weeks after tamoxifen treatment (Fig. 1*F*). These results suggest that PDK1-MerCre mice exhibited cardiac dysfunction as early as 1 week after tamoxifen treatment and LV remodeling at 4 weeks.

It was reported that PDK1-MCKCre showed marked reduction both in the heart size and in cardiac contractility (5). Since the *MCK* promoter directs expression of Cre recombinase before birth (5, 12), retardation of heart growth that was not proportional to somatic growth after birth might lead to cardiac dysfunction. However, the surface areas of caridomyocytes were not significantly different between PDK1-MerCre mice and control mice 1 week after tamoxifen treatment (Fig. 1*G*). Given that LV dysfunction was already observed as early as 1 week after tamoxifen treatment (Fig. 1 *C* and *D*), we suppose that reduction of cardiomyocyte size is not critically involved in the impairment of LV contraction observed in PDK1-MerCre hearts.

Increased Cardiomyocyte Apoptosis in PDK1-MerCre Mice. We next examined whether cardiomyocyte apoptosis was involved in the pathogenesis of heart failure in PDK1-MerCre mice. TUNEL staining revealed that the number of apoptotic cells was dramatically increased in PDK1-MerCre hearts 1 week after tamoxifen treatment (Fig. 2*A*). TUNEL-positive cells were cardiomyocytes, because these cells were positively stained with anti-sarcomeric α-actinin antibody (Fig. 2*B*). In addition, immunostaining revealed an increase in cardiomyocytes positively stained for cleaved caspase-3 in PDK1-MerCre hearts (Fig. 2*C*). The prevalence of TUNEL-positive cardiomyocytes was 1.14 ± 0.05% of total cardiomyocytes (Fig. 2*D*). Therefore, cardiomyocyte loss through apoptotic cell death may play an important role in the pathogenesis of heart failure in PDK1-MerCre mice.

In the hearts of PDK1-MerCre, the expression level of proapoptotic Bax was increased, whereas those of anti-apoptotic molecules such as Bcl-2 and Bcl-xL were unchanged (Fig. 2*E*). SGK1 has been reported to be functionally anti-apoptotic in the hearts (13). The basal level of phosphorylated SGK1 was reduced in PDK1-MerCre hearts (Fig. 2*F*). It has been reported that SGK1, in concert with Akt, mediates cell survival by phosphorylating and inactivating the Forkhead transcription factor FOXO3a (13, 14). FOXO3a is phosphorylated at Thr-32 and Ser-315 by SGK1, and Akt favors the phosphorylation of Thr-32 and Ser-253 (14). In PDK1-MerCre hearts, phosphorylation levels of FOXO3a at Thr-32 and Ser-253 were significantly decreased (Fig. 2*F*). Collectively, these results suggest that up-regulation of Bax protein and reduction of Akt and SGK1 activity were potentially involved in enhancing susceptibility of cardiomyocytes to apoptosis in PDK1-MerCre mice.

Overexpression of Bcl-2 Protein Prevented Cardiomyocyte Apoptosis and Partially Rescued Cardiac Dysfunction in PDK1-MerCre Mice. To examine whether cardiomyocyte apoptosis plays a causative role in the pathogenesis of heart failure in PDK1-MerCre mice, we crossed PDK1-MerCre with transgenic mice with cardiac-specific overexpression of Bcl-2 (Bcl2-Tg mice) (15). In PDK1-MerCre × Bcl2-Tg hearts, the number of TUNEL-positive cardiomyocytes was significantly decreased in comparison with PDK1-MerCre hearts (Fig. 2*G*), and the %FS showed partial but significant improvement (Fig. 2*H*). These results suggest that cardiac dysfunction is caused in part by cardiomyocyte loss through apoptosis in PDK1-MerCre mice.

Impairment of β-adrenergic Responsiveness in PDK1-MerCre Hearts. Incomplete restoration of cardiac function by prevention of cardiomyocyte apoptosis implies that some functional abnormalities persist in viable cardiomyocytes in PDK1-MerCre mice. To determine whether β-adrenergic responsiveness was changed in PDK1-MerCre hearts, we carried out Langendorff perfusion analysis in the hearts 1 week after tamoxifen treatment, and evaluated responsiveness to isoproterenol, a β-AR agonist, and forskolin, an activator of adenylate cyclase that increases cAMP independently

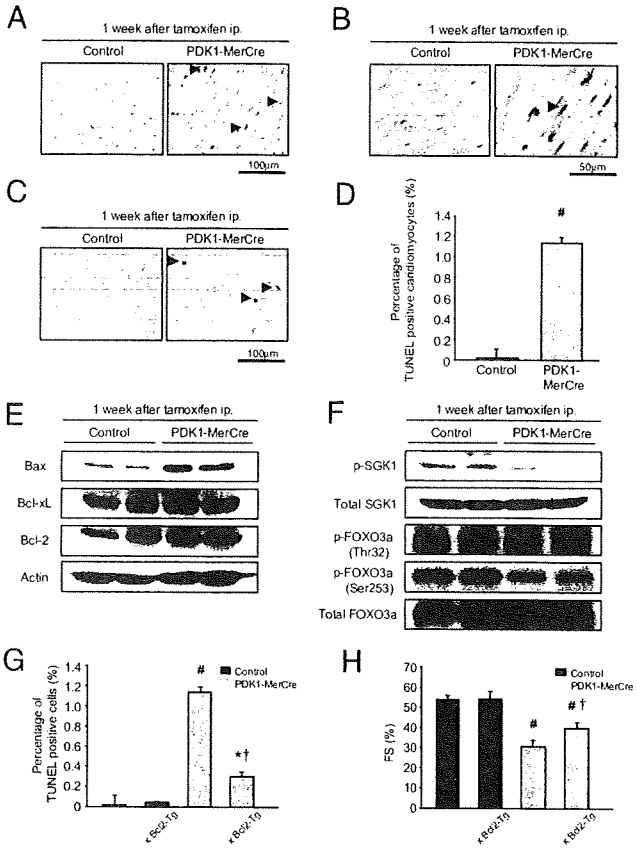

Fig. 2. Cardiomyocyte apoptosis in the pathogenesis of heart failure in PDK1-MerCre mice. (*A*) TUNEL staining. Arrowheads indicate TUNEL-positive cardiomyocytes. (*B*) Double staining for TUNEL staining (brown) and sarcomeric α-actinin (red). Arrowheads indicate TUNEL-positive cardiomyocytes. (*C*) Immunostaining for cleaved caspase-3. Arrowheads indicate cardiomyocytes positively stained for cleaved caspase-3. (*D*) Percentage of TUNEL-positive caridomyocytes. Values represent the mean ± SEM (3,000 cardiomyocytes in each group). #, $P < 0.01$ versus control group. (*E*) Immunoblot analysis of Bcl-2 family proteins in the hearts. (*F*) Immunoblot analysis of phosphorylated-SGK1 at Ser-78, total SGK1, phosphorylated-FOXO3a at Thr-32 or at Ser-253, and total FOXO3a in the hearts. (*G*) Percentage of TUNEL-positive caridomyocytes in control, Bcl2-Tg, PDK1-MerCre, and PDK1-MerCre × Bcl2-Tg mice. Values represent the mean ± SEM (3,000 cardiomyocytes in each group). #, $P < 0.01$ versus control group; *, $P < 0.05$, versus control group; †, $P < 0.01$ versus PDK1-MerCre group. (*H*) Measurement of fractional shortening of control, Bcl2-Tg, PDK1-MerCre, and PDK1-MerCre × Bcl2-Tg mice by echocardiography. Values represent the mean ± SEM of data from control mice (n = 10), control × Bcl2-Tg mice (n = 6), PDK1-MerCre mice (n = 10), and PDK1-MerCre × Bcl2-Tg mice (n = 6). #, $P < 0.01$ versus control mice. †, $P < 0.01$ versus PDK1-MerCre mice. FS, % of fractional shortening.

of β-AR. As shown in Fig. 3*A*, the baseline parameters of +dp/dt and −dp/dt were significantly lower in PDK1-MerCre mice than in control mice. Both isoproterenol and forskolin induced positive chronotropic and inotropic responses in control mice (Fig. 3*A*). However, PDK1-MerCre mice showed a significant reduction in the maximal changes in HR, +dP/dt, and −dP/dt after the stimulation of isoproterenol (1×10^{-8} M), compared with control mice (Fig. 3*B*). In contrast, the maximal changes in these parameters after the stimulation of forskolin (1×10^{-7} M) did not differ significantly between PDK1-MerCre and control mice (Fig. 3*B*). These results suggest that the responsiveness of β-AR is impaired in PDK1-MerCre mice.

Next, we measured the amount of β_1-AR in the membrane fraction by immunoblot analysis. In PDK1-MerCre hearts, the expression levels of β_1-AR in membrane fraction were markedly

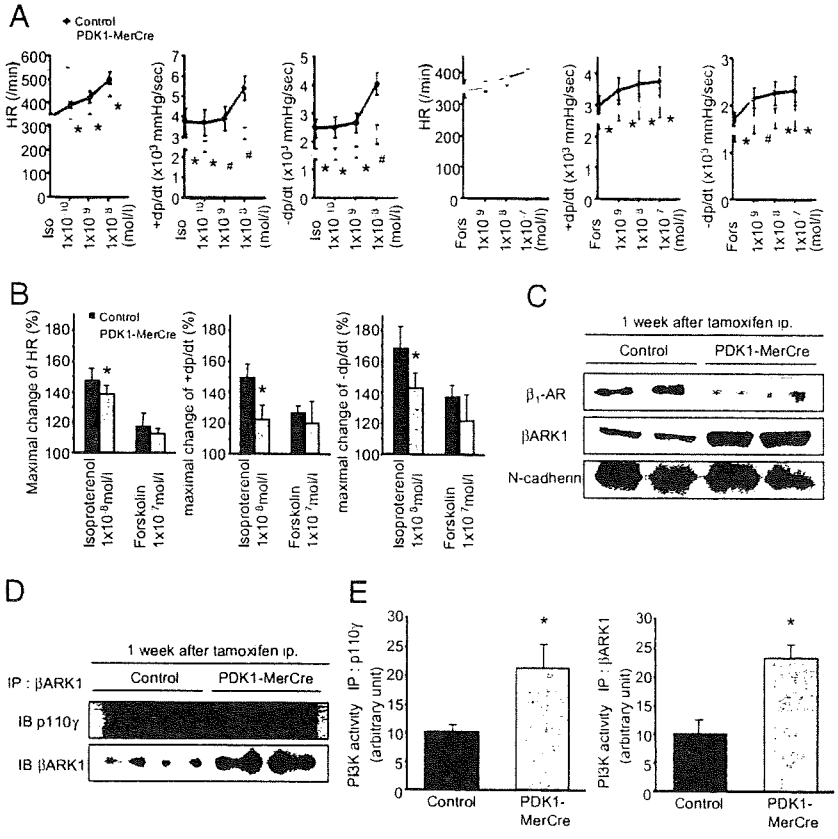

Fig. 3. Impaired β-adrenergic responsiveness in PDK1-MerCre mice. (*A*) Effects of isoproterenol and forskolin on heart rate, contraction, and relaxation in Langendorff-perfused mouse hearts 1 week after tamoxifen treatment. -dp/dt, maximum rate of LV pressure development; -dp/dt, maximum rate of LV pressure decline; HR, heart rate. Values represent the mean ± SEM. *, $P < 0.05$ versus control group, #, $P < 0.01$ versus control group. (*B*) The % changes in HR, -dP/dt, and -dP/dt before and after treatment with isoproterenol (1×10^{-8} M) or forskolin- (1×10^{-7} M) were calculated. Values represent the mean ± SEM. *, $P < 0.05$ versus control group. (*C*) Immunoblot analysis of β_1-AR and βARK1 in membrane fraction of the hearts. N-cadherin was used as an internal control for the amount of membrane protein. (*D*) Immunoblot analysis of βARK1-associated p110γ protein in the hearts. (*E*) Kinase assays for PI3-K activity. The hearts were subjected to immunoprecipitaion with antibody to p110γ, or βARK1, and the resulting precipitates were assayed for the kinase assay. PI3-K activity of control mice was adjusted to 10 arbitrary units.

down-regulated (Fig. 3*C*). Inversely, the amount of β_1-AR in cytosolic fraction was increased in PDK1-MerCre hearts, compared with control hearts, while the total amount of β_1-AR was unchanged (Fig. S3 *A* and *B*), suggesting that receptor internalization underlies β_1-AR down-regulation in membrane fraction of PDK1-MerCre hearts. In response to β-AR simulation, increased cAMP activates protein kinase A (PKA), which directly phosphorylates phospholamban (PLN) at Ser-16. PDK1-MerCre hearts showed a significant decrease in cAMP concentrations (Fig. S3*C*) and phosphorylation level of PLN at Ser-16 (Fig. S3*D*), compared with control hearts. Phosphorylated PLN dissociates from sarcoplasmic reticulum Ca^{2+}-ATPase2 (SERCA2) and thereby enhances Ca^{2+} uptake by SERCA2, which leads to enhancement of cardiac contractility (2). These results suggest that, in PDK1-MerCre hearts, robust β_1-AR internalization leads to contractile dysfunction.

It has been reported that phosphorylation of β-AR by β-AR kinase 1 (βARK1, commonly known as G protein-coupled receptor kinase 2) regulates receptor internalization (16). In the hearts of PDK1-MerCre mice 1 week after tamoxifen treatment, the expression levels of βARK1 (Fig. 3*C*) and βARK1-associated p110γ, a catalytic subunit of PI3-Kγ, were increased (Fig. 3*D*). Notably, PI3-K activity immunoprecipitated with antibodies to either p110γ or βARK1 was enhanced (Fig. 3*E*) in PDK1-MerCre hearts. βARK1 forms complex with PI3-Kγ through the phosphoinositide kinase (PIK) domain, and protein kinase activity of PI3-Kγ in this complex is required for receptor internalization (17). Therefore, these results suggest that enhanced PI3-Kγ activity in PDK1-MerCre hearts increases βARK1/PI3-Kγ complex formation, and that βARK1 phosphorylates β-AR to cause robust receptor internalization.

Disruption of βARK1/PI3-Kγ Complex Restored β-AR Internalization and Partially Rescued Cardiac Dysfunction in PDK1-MerCre Mice. To corroborate that enhanced PI3-Kγ activity promotes β-AR internalization by forming complex with βARK1 and that robust β-AR internalization causes cardiac dysfunction, we examined whether disruption of the βARK1/PI3-Kγ complex normalizes β-AR trafficking and improves cardiac function in PDK1-MerCre mice. For that purpose, we crossed PDK1-MerCre mice with transgenic mice harboring cardiac-specific overexpression of PIK domain (PIK-Tg mice) (16), which competitively inhibits the association between βARK1 and PI3-Kγ. The amount of βARK1-associated p110γ protein was significantly decreased in PDK1-MerCre × PIK-Tg mice, compared with PDK1-MerCre mice (Fig. 4*A*). Importantly, βARK1-associated PI3-K activity was markedly decreased in PDK1-MerCre × PIK-Tg mice, compared with PDK1-MerCre mice (Fig. 4*B*, *Lower*), although total PI3-Kγ activity remained elevated (Fig. 4*B*, *Upper*). As a consequence, in PDK1-MerCre × PIK-Tg mice 1week after tamoxifen treatment, the expression levels of β_1-AR in membrane fraction were restored (Fig. 4*C*). The %FS in echocardiographic examination showed partial but significant improvement (Fig. 4*D*). Overexpression of PIK domain did not influence cardiomyocyte apoptosis, because the prevalence of TUNEL-positive cardiomyocytes (Fig. 4*E*), as well as the amount of cleaved poly(ADP-ribose) polymerase, Bax, and phosphrylated FOXO3a (Fig. S4), was unchanged in PDK1-MerCre hearts. In addition, overexpression of Bcl-2 protein did not influence β-adrenergic response, because the amount of βARK1-associated p110γ protein (Fig. 4*A*), βARK1-associated PI3-K activity (Fig. 4*B*), the expression levels of membranous β_1-AR (Fig. 4*C*), as well as cAMP concentration and phosphorylation levels of PLN at Ser-16 (Fig. S5), were unchanged in PDK1-MerCre hearts. These results suggest that enhancement of βARK1-associated PI3-Kγ activity induces robust β-AR internalization, and thereby contributes to cardiac dysfunction, independently of cardiomyocyte apoptosis, in PDK1-MerCre mice.